Mon. Not. R. Astron. Soc. **366,** 1265–1288 (2006) doi:10.1111/j.1365-2966.2005.09916.x

CENSORS: A Combined EIS–NVSS Survey of Radio Sources – II. Infrared imaging and the *K*–*z* relation

M. H. Brookes,[1]⋆ P. N. Best,[2] R. Rengelink[2] and H. J. A. Röttgering[2]

[1]*Institute for Astronomy, Royal Observatory Edinburgh, Blackford Hill, Edinburgh EH9 3HJ*
[2]*Sterrewacht Leiden, Postbus 9513, 2300 RA Leiden, the Netherlands*

Accepted 2005 November 18. Received 2005 November 3; in original form 2005 August 24

ABSTRACT

The Combined EIS–NVSS Survey of Radio Sources (CENSORS) is a 1.4-GHz radio survey selected from the National Radio Astronomy Observatories (NRAO) Very Large Array (VLA) Sky Survey (NVSS) and complete to a flux density of 7.2 mJy. It targets the European Southern Observatory (ESO) Imaging Survey (EIS) Patch D, which is a 3×2-deg^2 field centred on right ascension $09^{\rm h}51^{\rm m}36\overset{\rm s}{.}0$ and declination $-21^\circ 00' 00''$ (J2000). This paper presents *K*-band imaging of 142 of the 150 CENSORS sources. The primary motivation for beginning infrared imaging of the sample was to identify the host galaxies of ∼30 per cent of sources for which the EIS *I*-band imaging failed to produce a likely candidate. In addition, *K*-band magnitudes allow photometric redshift estimation and $I - K$ colours aid the identification of host galaxies (which are typically old, red ellipticals). Of the sources observed in the *I* and *K* bands, four remain undetected, possibly indicating high redshifts for the host galaxies, and eight involve complicated radio structures, or several candidate host galaxies, which have yet to be resolved. Thus, the host galaxy identifications are brought to 92 per cent completeness.

In conjunction with spectroscopic observations, the *K*-band magnitudes have been aperture corrected and used to establish a *K*–*z* relation for the CENSORS radio galaxies. This relation is of interest because of its variation, at $z > 1$, between radio surveys of different flux-density limit. Establishing this relation for CENSORS may shed light on the origin of this variation and will allow an appropriate *K*–*z* redshift estimator for any CENSORS source which remains without a spectroscopic redshift. It is shown that whilst the *K*–*z* relation for CENSORS is fainter than that of 3CRR at all redshifts, it agrees well with that of 7C over all redshifts studied.

Key words: surveys – galaxies: active – radio continuum: galaxies.

1 INTRODUCTION

There are many important questions regarding radio-loud active galactic nucleus (AGN) astrophysics which remain unanswered. Just a few examples are: What causes the radio loudness in some AGN? How does this vary with host galaxy/black hole mass or environment? What is the underlying difference between Fanaroff & Riley (1974) Class I and Class II radio sources (FRI/II)? How do radio sources evolve individually and as a population and how are these linked to the global star formation history of the Universe, and structure formation more generally? One approach to start addressing these questions is the development of large, well-defined samples of radio sources, for which the redshifts are known.

⋆E-mail: Mairi.H.Brookes@jpl.nasa.gov

Flux-density-limited surveys offer samples for which the selection effects can be understood, thus making interpretation relatively simple. However, a disadvantage arises from the degeneracy of radio luminosity and redshift due to the flux-density limit. Because of this it is useful to have several radio surveys, with a range of flux-density limits, which together span a wide range across the radio luminosity–redshift (*P*–*z*) plane. Producing a radio survey which would extend the current coverage of the *P*–*z* plane was one of the primary motivations for developing the Combined EIS–NVSS Survey of Radio Sources (CENSORS; Best et al. 2003; hereafter Paper 1). This 150-source sample is complete to 7.2 mJy at 1.4 GHz and covers a field of $2 \times 3\,{\rm deg}^2$ on the southern sky. The sample was selected from the National Radio Astronomy Observatories (NRAO) Very Large Array (VLA) Sky Survey (NVSS) (Condon et al. 1998) in a region overlapping the European Southern Observatory (ESO) Imaging Survey Patch D (EISD) (Nonino et al. 1999; EIS). The EIS *I*-band data ($I \lesssim 23.5$) were then used to identify host

galaxies for the radio sources. In this paper, the K-band imaging of the CENSORS sample is described.

The first motivation for these observations is to identify host galaxies which were not identified optically. In Paper 1, around 70 per cent of the sources were associated with host galaxies which were identified from the I-band imaging of the EIS. However, in order that this sample may be useful, the remaining host galaxies must be identified. To detect the remaining host galaxies, it is beneficial to observe at longer wavelengths because radio source host galaxies are typically hosted by old, elliptical galaxies (e.g. Best, Longair & Röttgering 1998) and these are significantly brighter at longer wavelengths. This is particularly true at high redshifts where the optical waveband observes the redshifted rest-frame ultraviolet. In addition, where there was doubt over an I-band candidate host galaxy or where there were two galaxies considered likely host candidates, the K band allows a $I - K$ colour to be established and which can be used to aid the identification process.

In addition to observing those sources without host galaxy identifications, there is motivation to observe the entire sample in order to establish K-band magnitudes for radio galaxies with the CENSORS sample. Given the experience of previous radio surveys, it is unlikely that the CENSORS sample can be brought to 100 per cent spectroscopic completeness in a short period of time and so photometric redshift estimation methods are required in this project. The K–z relation could be used as a first estimate of the redshift for a non-spectroscopically identified host galaxy. As described above, K-band observations of radio galaxies are dominated by emission from the old stellar population. Since this emission does not change as rapidly with evolution of the stellar population as emission at shorter wavelengths, and radio galaxy hosts form a fairly homogenous sample of objects, a tight relation between K-band magnitude and redshift exists for radio galaxies (Lilly & Longair 1984; Eales & Rawlings 1996; Best et al. 1998).

However, there is uncertainty in the understanding of the dependence of the K–z relationship upon radio luminosity. When the K–z relation was first investigated, using solely the 3CRR sample, it was shown that the relation matched the predictions of passive evolution of an old, stellar population and this was interpreted as showing that the high-redshift radio galaxies evolved into the low-redshift radio galaxies (Lilly & Longair 1984). However, subsequent observations have shown that this cannot be the case. First, the high-redshift galaxies reside in rich environments, whereas the low-redshift galaxies are found to be isolated or in small groups (Best 2000, and references therein). In addition, the K–z relations for the 3CRR and 6C [the 6CE survey of Eales (1985) and the filtered 6C* survey of Blundell et al. (1998)] samples agree at low redshift but show a mean offset of $\sim$0.6 mag at redshifts of $z > 1$, the 3CRR galaxies being brighter in K (see Eales & Rawlings 1996; Jarvis et al. 2001; Inskip et al. 2002). Willott et al. (2003) added the 7C survey to this comparison and showed that the 7C and 3CRR surveys are offset in K-band magnitude at all redshifts and that small numbers of sources in the low-redshift bins of the 6C surveys lead to large errors, thus showing that they too may be consistent with a gradual offset in K as a function of flux-density limit. The CENSORS survey is approximately 12 times fainter again than the 7C survey (for a typical radio galaxy spectrum of $S \propto \nu^{-0.75}$). In order to use a K–z relation as a first estimate of the redshift for non-spectroscopically identified CENSORS sources, it is therefore necessary to establish a K–z relationship for CENSORS, rather than blindly applying the relationship developed with other samples of higher flux-density limit.

CENSORS may also be able to help resolve the puzzle. There are two possible interpretations for the varying K–z relation result. First, the most luminous radio sources could suffer a significant contribution, from activity associated with the AGN, to the K band. Secondly, at high redshifts the more powerful radio sources may be associated with more massive galaxies (Best et al. 1998). CENSORS can be used to test between these since in the first case contamination could be from a partially obscured nucleus or emission line contributions in the 3CR sources (Eales et al. 1997). In this case, little change is expected in K magnitude between the 6C and CENSORS and this result would have implications for interpretation of SEDs of 3CRR radio galaxies in terms of stellar populations. The second case might be motivated by suggesting that the most powerful radio sources are powered by the most massive black holes and, since the black hole mass is roughly proportional to the galaxy bulge mass (Kormendy & Gebhardt 2001), hence are hosted by the most massive galaxies. In this case CENSORS galaxies would be fainter than 6C in the K band and this would have important implications for the evolution of fuelling of RGs (in order that the low- and high-redshift results can be reconciled).

The development of the CENSORS sample by identifying host galaxies and targeting them with spectroscopic observations has been carried out over the last 4 yr. The basic radio data and I-band results are presented in Paper 1. This paper presents the K-band imaging and will be referred to as Paper 2, whilst the spectroscopic observations will be presented in Brookes et al. (in preparation; Paper 3). Note that some of the results of the spectroscopic observations are referenced in this paper in order that aperture corrections to the K-band magnitudes may also be presented here. In addition to these three data papers, an investigation of the cosmological evolution of radio sources has been carried out. This was the primary scientific goal of developing this sample and in Brookes et al. (in preparation; Paper 4) a study of that topic will be presented.

The layout of the current paper is as follows. Section 2 describes the observations, data reduction methods and photometric analysis of the data. Section 3 presents the results of these observations and includes tabulated photometric measurements and the K-band images of a subsample of the CENSORS sources. Section 4 describes the aperture corrections to the observed K-band magnitudes for those sources with a spectroscopic redshift (presented in Paper 3). Section 5 presents the CENSORS K–z relation for radio galaxies and a summary of results and conclusions is given in Section 6. Throughout this paper, the following cosmological parameters are adopted: $H_0 = 70\,\mathrm{km\,s^{-1}\,Mpc^{-1}}$, $\Omega_\mathrm{M} = 0.3$ and $\Omega_\Lambda = 0.7$.

2 IMAGING

2.1 Observations

The K-band imaging of 142 of the 150 CENSORS sources was carried out over several runs using UFTI on United Kingdom Infrared Telescope (UKIRT) (2001, 2002), ISAAC on the Very Large Telescope (VLT) (2002) and IRIS2 on the Anglo-Australian Telescope (AAT) (2003, 2004), the latter three runs being done in service mode. UFTI has a 1024 $\times$ 1024 HgCdTe array and a plate scale of 0.09 arcsec pixel^{-1}, giving a field of 92 $\times$ 92 arcsec^2; ISAAC has a 1024 $\times$ 1024 Rockwell detector, with a pixel scale of 0.1484 arcsec pixel^{-1} and covering a field of 2.5 $\times$ 2.5 arcmin^2; IRIS2 again has a 1024 $\times$ 1024 Rockwell HAWAII-1 HgCdTe detector with 0.446 arcsec pixel^{-1}, giving a field of view of 7.7 $\times$ 7.7 arcmin^2. All observations were made using a nine-point jitter

Table 1. Details of observing runs for K-band imaging of CENSORS. *Included in this data set are two observations made in service mode: CENSORS 51 and 98 in 2002 November 27 and 2003 February 4, respectively.

Run	Date	Telescope (instrument)	Nights photometric
1	2001/02/03–2001/02/06	UKIRT (UFTI)	4
2*	2002/04/19–2002/04/26	UKIRT (UFTI)	2
3	2002/03/16, 2002/04/15	VLT (ISAAC)	2
4	2003/06/06, 2003/06/13	AAT (IRIS2)	0
5	2003/01/20–2003/01/23	AAT (IRIS2)	0
6	2004/04/01–2004/04/03	AAT (IRIS2)	0

pattern of offset exposures in order to produce a good flat-field and to allow removal of the rapidly varying infrared (IR) sky background. Typical seeing for these observations were: UKIRT 2001: 0.8 arcsec; UKIRT 2002: 0.65 arcsec; VLT 2002: 0.5 arcsec, AAT 2003: 0.8 arcsec, AAT 2004: 1–2.5 arcsec. The K' improves on the K band (for non-*IR* optimized telescopes) by being slightly narrower in order to reduce thermal background from warm ground-based telescopes. All the telescopes (other than UKIRT) had a K' (or similar) filter available and this was used. However, since photometric calibration was done using K magnitudes and since the colour dependence of the correction from K' to K ($\leqslant$0.01 mag) is much smaller than the errors, the difference is ignored hereafter, and all filters are referred to as K for simplicity. The details of these runs are given in Table 1 and are associated with a run number, given in this table, by which they will be referred to later.

Observations of standard stars were made on photometric nights. These observations were generally five-point jitter patterns and were reduced by the same prescription as the science targets.

2.2 Data reduction

Data reduction was performed identically for observations from all observing runs. It was done using the DIMSUM task[1] in the IRAF data reduction package (Tody 1986, 1993). Dark frames were subtracted. A flat-field was produced by averaging over images from the full jitter pattern, and was used to normalize the images. These images were sky-subtracted and cosmic rays were removed. Following this they were registered and combined in the 'reduce' task by reference to the brightest unresolved objects in the frame. A bad pixel map was produced and used to remove bad pixels in each image, before the final combined image was produced.

2.3 Astrometry and host galaxy identification

Accurate astrometry is essential in order to correctly identify the counterparts to the CENSORS radio sources. This was done using IDL by comparing bright, but unsaturated stars with those in the EIS I-band catalogue. The procedure in IDL fits pixel scale, image rotation and reference right ascension (RA) and declination (Dec.). The astrometry is typically certain to $\lesssim$0.1 arcsec relative to the I-band images. The I-band images themselves are matched to the radio frame with an astrometric accuracy of within 0.2 arcsec (Nonino et al. 1999). However, note that for those sources for which a only a faint detection has been made the measured position may be much less certain ($\sim$1 arcsec).

[1] DIMSUM is the 'Deep Infrared Mosaicking Software' package, developed by Eisenhardt, Dickinson, Standford and Ward.

2.4 Photometry

On photometric nights, the K-band magnitudes of standard stars were used to determine the zero-point of the images for the night. The standards were taken from the Faint UKIRT JHK Standards list (Casali & Hawarden 1992) and were chosen on the basis of their brightness and proximity to the CENSORS target field. They include: FS3, FS19, FS20, FS27, FS103, FS121, FS124, FS125, FS126 and FS128. The calculated zero-point was then used to calculate the magnitude of the target sources from their counts. The zero-point varied by $\sim$0.05 mag between different standard stars and this was taken to be the error in this figure.

The zero-point may also be determined for non-photometric images using stars within the field of view from which the K-band magnitude is known. These magnitudes are obtained either with reference to previous photometric images or from the two-Micron All Sky Survey Catalogue of Point Sources (2MASS[2]). When 2MASS was used, only stars brighter than $K = 14.3$ were used for calibration and the zero-point was taken to be the average of those determined for the calibration sources. The error was taken to be the standard deviation of those zero-points.

2.4.1 Aperture radius

Since the observed sources span a wide range in redshifts (cf. Paper 3), apertures of the same radius on the sky, will not correspond to the same physical radius and so, ultimately, it is desirable to correct the measured K-band magnitudes to a standard physical aperture, on the basis of the redshift of the source. In addition, more ad hoc problems occur, such as neighbouring sources, which prevent a large aperture measurement being possible. In order to achieve this in a simple and yet flexible manner, the photometric analysis has been performed for several apertures of different radius, where possible.

For targets observed at UKIRT, 1, 1.5, 2.5 and 4.5 arcsec radius apertures were used. Targets observed at the AAT were brighter and therefore, typically, closer. A combination of the fact that these sources were more likely to be extended than the UKIRT targets and the fact that IRIS2 has larger pixels meant that a 1-arcsec aperture was usually unpractical. So these targets were measured with only the 1.5-, 2.5- and 4.5-arcsec apertures. Some targets required smaller apertures due to the presence of nearby sources or because they were very weak and this was the only way to obtain an accurate measurement.

2.4.2 Magnitudes and errors

The counts detected for a source were determined using the 'phot' task in IRAF. The 'phot' task measures counts in circular apertures and calculates sky counts from an annular aperture. It was applied to the target, then $\sim$10 identical apertures are placed on blank patches of sky near the target. These data were then used to measure the Gaussian error in the source counts, the Gaussian error in the sky counts and the standard deviation of the residual (post-sky subtraction count) in the blank apertures. This residual tells us whether the error in the sky background is dominated by the variance of the sky background within an aperture or by the varying sky background over the image. If the residual error is greater or of the order of the sky variance within an aperture, which in almost all cases it was,

[2] This work makes use of data products from the 2MASS, which is a joint project of the University of Massachusetts and the Infrared Processing and Analysis Center/California Institute of Technology, funded by the National Aeronautics and Space Administration and the National Science Foundation.

Table 2. Details of *K*-band observations of CENSORS and results. Both the CENSORS and EISD are listed to allow easy reference to Paper 1 and for archival purposes. The observation runs are listed and described in detail in Table 1. The *K*-band magnitudes are listed, as measured in apertures of radii 1, 1.5, 2.5 and 4.5 arcsec. In some cases a smaller aperture was required and these are listed in the 'Other' column. The 2σ *K*-band limit, for undetected sources, is based upon a 1 arcsec radius aperture. For all magnitudes, the errors (in 1/100ths of a magnitude) are given in brackets.

CENSORS	EISD	Observation runs	Exposure time (s)	RA (^{h} ^{m} ^{s})	Dec. ($^\circ$ $'$ $''$)	1 arcsec	1.5 arcsec	2.5 arcsec	4.5 arcsec	Other	2σ limit
1	1	6	499.2	09 51 29.19	−20 50 30.90	–	18.13(25)	–	–	–	–
2	2	2	1080	09 46 50.20	−20 20 44.04	19.00(12)	18.69(27)	–	–	–	–
3	3	6	374	09 50 31.41	−21 02 44.32	–	17.07(12)	16.67(13)	–	–	–
4	6	6	1020	09 49 53.30	−21 56 20.66	–	18.20(21)	17.82(25)	–	–	–
5	8	6	1080	09 53 44.52	−21 36 01.05	–	19.35(29)	–	–	–	–
6	7	5	1080	09 51 43.61	−21 23 58.57	–	16.44(16)	16.18(19)	15.99(27)	–	–
7	10	6	1080	09 45 56.69	−21 16 53.47	–	18.49(28)	17.79(33)	–	–	–
8	11	–	–			–	–	–	–	–	–
9	12	5	392	09 49 35.54	−21 56 24.06	–	16.78(16)	16.30(17)	16.11(25)	–	–
10	16	4	1620			16.46(06)	16.16(06)	15.98(07)	15.93(08)	–	–
11	15	6	432	09 53 29.56	−20 02 11.95	–	18.91(33)	–	–	–	–
12	18	6	540	09 46 41.17	−20 29 26.19	–	19.13(26)	–	–	–	–
13	20	1, 2	1080, 1912	09 54 29.00	−21 56 54.85	19.87(20)	19.86(16)	–	–	–	–
14	21	1	1080	09 54 47.65	−20 59 44.04	19.04(15)	18.51(11)	18.13(17)	17.75(24)	–	–
15	22	6	480			–	–	–	–	–	19.0
16	23	1	1080	09 57 51.41	−21 33 22.47	19.85(33)	–	–	–	–	–
17	24	6	540	09 52 43.11	−19 58 21.90	–	18.07(20)	18.02(30)	–	–	–
18	25	5	600	09 55 13.59	−21 23 02.89	–	13.85(15)	13.34(15)	13.02(15)	–	–
19	27	1	1080	09 53 30.52	−21 36 02.76	18.66(16)	18.26(13)	17.92(19)	17.62(33)	–	–
20	30	1, 2	1080, 2376							–	19.4
21	28	6	1080	09 47 59.02	−21 21 51.65	–	18.53(22)	18.35(31)	–	–	–
22	29	1	1080	09 57 30.83	−21 32 39.18	18.07(13)	17.87(18)	18.03(35)	–	–	–
23	31	1, 2	1080, 706	09 56 29.93	−20 01 32.46	19.65(12)	19.24(21)	18.76(27)	–	–	–
24	32	1, 3	1080, 2100	09 54 38.32	−21 04 24.50	19.88(18)	19.69(26)	19.43(39)	–	–	–
25	34	1, 2	1080, 1426	09 48 04.06	−21 47 36.06	19.75(13)	19.45(18)	18.85(23)	18.42(27)	–	–
26	36	1, 3	1080, 2100			–	–	–	–	–	19.8
27	44	5	1080	09 51 49.84	−21 24 58.08	–	16.39(17)	16.03(19)	15.87(22)	–	–
28	38	1	1080	09 46 32.14	−20 26 15.36	16.72(06)	16.38(07)	16.11(08)	15.98(10)	–	–
29	39	5	373.8	09 48 15.81	−21 40 06.95	–	17.94(22)	17.29(23)	–	–	–
30	40	–	–			–	–	–	–	–	–
31	41	2	1080	09 45 19.78	−21 42 38.04	18.00(09)	17.84(09)	17.73(13)	–	–	–
32	43	1	1080	09 51 40.85	−20 11 16.11	18.37(13)	17.91(18)	17.80(29)	–	–	–
33	45	1	1080	09 53 05.00	−20 44 13.88	19.17(12)	19.05(28)	18.91(25)	–	–	–
34	47	2	540	09 47 53.59	−21 47 19.25	18.85(19)	18.78(12)	18.64(38)	–	–	–
35	48	5	990	09 54 52.47	−21 19 29.53	–	16.93(10)	16.59(12)	16.53(19)	–	–
36	51	6	1080	09 49 33.32	−21 27 06.77	–	18.89(21)	–	–	–	–
37	52	1, 2	1080, 950	09 49 19.55	−21 51 33.92	19.63(21)	19.45(26)	–	–	–	–
38	53	1	1080	09 51 16.89	−20 56 37.01	17.49(09)	17.36(12)	17.25(15)	17.03(23)	–	–
39	54	6	540	09 48 36.18	−21 06 22.40	–	18.04(27)	17.63(33)	–	–	–
40	55	1, 2	1080, 864	09 50 58.98	−21 14 23.80	18.33(11)	18.09(12)	17.88(20)	18.00(30)	–	–
41	58	5	294	09 49 18.23	−20 54 46.12	–	16.08(14)	15.44(18)	15.07(19)	–	–
42	60	6	1080			–	–	–	–	–	18.8
43	64	6	540	09 52 59.15	−21 48 41.70	–	17.54(19)	–	–	–	–
44	62	6	447			–	18.49(25)	17.98(30)	–	–	–
45	66	6	495.6	09 57 42.98	−20 06 36.82	–	17.28(06)	17.04(11)	16.85(20)	–	–
46	65	6	540	09 54 03.06	−20 25 12.90	–	17.44(10)	17.15(10)	17.25(17)	–	–
47	63	5	428.4	09 47 03.36	−20 50 00.72	–	17.32(22)	16.97(20)	16.50(21)	–	–
48	68	6	540	09 54 28.38	−20 39 28.11	–	18.17(25)	17.67(25)	–	–	–
49	67	5	840	09 53 23.25	−20 13 44.84	–	16.43(19)	16.09(21)	15.88(24)	–	–
50	69	1	1080	09 52 12.71	−21 02 36.53	19.03(17)	18.74(21)	–	–	–	–
51	75	1, 2	1080, 1080	09 51 22.98	−21 51 53.36	20.56(32)	20.70(31)	–	–	–	–
52	72	1	1080	09 45 42.60	−21 15 43.80	18.93(15)	18.83(18)	18.61(24)	–	–	–
53	76	5	413.4	09 51 32.44	−21 00 29.09	–	16.28(19)	15.60(17)	–	–	–
54	74	5	490	09 53 20.67	−21 43 59.21	–	15.29(09)	14.72(09)	14.25(10)	–	–
55	71	6	540	09 49 30.80	−20 23 34.47	–	18.51(65)	16.89(10)	16.67(15)	–	–
56	78	6	1080	09 50 43.20	−21 26 42.57	–	18.34(15)	17.99(30)	–	–	–
57	80	6	1080	09 51 21.08	−21 29 54.35	–	18.49(14)	18.18(15)	17.92(26)	–	–
58	79	1	1080			20.90(50)	–	–	–	–	–

Table 2 – *continued*

CENSORS	EISD	Observation runs	Exposure time (s)	RA (^{h} ^{m} ^{s})	Dec. ($^\circ$ $'$ $''$)	1 arcsec	1.5 arcsec	2.5 arcsec	4.5 arcsec	Other	2σ limit
59	81	2	540	09 48 42.49	−21 52 24.60	18.26(08)	18.27(21)	–	–	–	–
60	83	6	1080	09 51 48.71	−20 31 53.23	–	19.13(29)	18.55(26)	–	–	–
61	82	1	1080	09 48 01.98	−20 09 11.92	19.05(15)	18.82(19)	18.84(37)	–	–	–
62	84	6	540	09 49 45.90	−21 50 06.34	–	17.41(19)	–	–	–	–
63	88	5	990	09 45 29.64	−21 18 51.52	–	16.58(16)	16.38(20)	16.25(23)	–	–
64	85	1, 2	1080, 1912			–	–	–	–	–	19.1
65	87	6	463.2	09 57 26.04	−20 13 04.54	–	17.77(16)	16.95(22)	–	–	–
66	90	6	540			–	–	–	–	–	18.4
67	89	6	540	09 57 31.81	−21 20 30.45	–	16.95(15)	16.32(16)	16.05(17)	–	–
68	91	6	540			–	16.91(13)	–	–	–	–
69	92	6	1080			–	–	–	–	–	18.6
70 A	124	4	1620			18.34(07)	17.88(07)	17.50(10)	17.35(08)	–	–
B						18.12(09)	17.81(09)	17.69(09)	17.63(17)	–	–
C						19.18(13)	18.87(17)	18.90(23)	–	–	–
D						18.94(08)	18.49(09)	18.02(13)	17.55(17)	–	–
E						18.17(12)	17.73(13)	17.38(16)	17.20(25)	–	–
71	93	1, 2	1080, 4190	09 55 41.88	−20 39 38.17	20.38(15)	20.00(17)	–	–	–	–
72	97	1	1080	09 49 26.00	−20 37 23.70	18.88(15)	18.55(13)	18.04(19)	–	–	–
73	94	1	1080	09 56 28.09	−20 48 44.81	18.92(19)	18.57(20)	18.34(26)	17.80(18)	–	–
74	96	4	1620			18.57(15)	18.05(14)	17.55(17)	17.01(23)	–	–
75	98	5	630	09 45 26.95	−20 33 53.32	–	15.93(12)	15.32(13)	–	–	–
76	102	5	455	09 57 46.11	−21 23 27.87	16.43(24)	15.87(24)	15.47(24)	15.28(24)	–	–
77	104	1, 2	1080, 1026	09 49 42.95	−20 37 45.03	19.33(21)	19.01(25)	18.68(33)	–	–	–
78	107	5	624	09 55 59.31	−20 42 53.15		17.22(24)	16.85(29)	–	–	–
79	106	6	1080	09 45 48.55	−21 59 06.50	–	18.10(22)	17.63(24)	17.37(23)	–	–
80	110	5	1152	09 54 53.25	−21 15 13.29	–	15.69(12)	15.24(13)	14.77(14)	–	
81	105	6	753.6			–	–	–	–	–	18.7
82	113	5	540			–	–	–	–	–	18.4
83	116	6	540	09 51 29.71	−20 16 42.24	–	16.71(15)	–	–	–	–
84	103	4	1620	09 55 43.54	−21 25 27.55	18.47(11)	–	–	–	–	–
85	112	4	1620			–	–	–	–	–	20.1
86	120	6	1080	09 48 04.28	−20 34 35.19	–	17.74(15)	–	–	–	–
87	111	1, 4	1080, 1620			–	–	–	–	–	20.2
88	119	–	–			–	–	–	–	–	–
89	117	1, 2	1080, 853	09 53 09.89	−20 01 17.57	19.56(15)	19.53(27)	–	–	–	–
90	114	1, 2, 4	1080, 1998, 1620	09 47 27.10	−21 26 34.84	–	–	–	–	–	20.2
91	127	6	866.7	09 48 22.25	−21 05 08.49	–	18.57(29)	–	–	–	–
92	122	6	540	09 52 55.98	−20 51 44.60	–	16.71(21)	16.47(25)	–	–	–
93	132	5	540	09 46 19.16	−20 37 58.53	16.81(14)	16.21(15)	15.65(18)	–	–	–
94	125	1, 3	1080, 2100	09 45 20.96	−20 43 19.18	–	–	–	–	19.58(09)[0.5]	–
95	123	5	720	09 54 21.59	−21 48 06.55	–	14.33(10)	13.74(10)	13.25(10)	–	–
96	131	1, 3	1080, 2100	09 49 26.06	−20 05 19.86	20.59(20)	20.40(26)	20.02(39)	–	–	–
97	126	2	540	09 54 36.24	−21 44 30.95	19.30(10)	19.32(19)	–	–	–	–
98	130	2	2808	09 49 35.19	−21 58 10.52	19.30(25)	18.93(29)	18.13(30)	17.14(28)	–	–
99	133	6	540	09 57 02.40	−21 56 50.60	–	17.36(17)	16.61(16)	16.18(22)	–	–
100	136	6	918.6	09 50 48.52	−21 54 55.53	–	–	–	–	–	18.8
101	139	6	1080	09 52 50.45	−21 31 48.24	–	18.38(26)	18.03(34)	–	–	–
102	134	5	784	09 46 49.49	−21 16 46.84	17.02(23)	16.47(22)	15.97(23)	–	–	–
103	56	1, 4	1080, 1620			–	–	–	–	–	20.2
104	145	6	979.8	09 57 39.08	−20 03 19.98	–	17.96(11)	17.67(14)	17.28(21)	–	–
105	138	1, 2	1080, 3170	09 47 24.54	−21 05 02.52	20.70(28)	–	–	–	–	–
106	142	6	540	09 56 07.13	−20 05 44.04	–	18.64(29)	–	–	–	–
107	148	6	540	09 45 38.10	−21 11 13.59	–	16.67(13)	16.32(13)	–	–	–
108	153	5	315	09 56 49.86	−20 35 26.15	–	15.58(15)	15.15(16)	14.92(20)	–	–
109	154	2	540	09 52 10.86	−20 50 08.85	17.59(06)	17.35(09)	17.09(14)	17.05(27)	–	–
110	141	–	–			–	–	–	–	–	–
111	149	5	780	09 47 44.79	−21 12 23.32	–	16.70(20)	16.24(22)	15.94(23)	–	–
112	146	–	–			–	–	–	–	–	–
113	150	6	1080	09 47 10.36	−20 35 52.22	–	18.03(22)	17.80(25)	–	–	–
114	166	6	1080	09 56 04.52	−21 44 36.66	–	19.23(34)	–	–	–	–
115	155	5	315	09 57 24.89	−20 22 42.48	–	16.20(20)	15.68(20)	15.22(23)	–	–
116	143	6	1414.8	09 57 35.46	−20 29 35.46	–	18.39(29)	18.23(27)	–	–	–

Table 2 – *continued*

CENSORS	EISD	Observation runs	Exposure time (s)	RA (^{h} ^{m} ^{s})	Dec. ($^\circ$ $'$ $''$)	1 arcsec	1.5 arcsec	2.5 arcsec	4.5 arcsec	Other	2σ limit
117	165	6	1080	09 54 10.58	−21 58 01.13	–	18.85(26)	18.31(31)	–	–	–
118	161	1, 3	1080, 2100	09 47 48.46	−20 48 35.28	19.82(15)	19.60(18)	19.59(28)	–	–	–
119	157	1	1080	09 49 02.22	−21 15 04.76	18.60(10)	18.16(11)	17.89(11)	17.85(32)	–	–
120	159	6	540	09 53 57.51	−20 36 50.74	–	17.68(19)	–	–	–	–
121	164	5	164.85	09 52 01.26	−20 24 56.50	–	15.85(15)	15.33(16)	14.86(17)	–	–
122	156	5	315	09 56 37.20	−20 19 05.70	–	15.67(18)	15.12(18)	14.62(19)	–	–
123	173	6	540	09 54 31.08	−20 35 37.14	–	17.72(12)	17.36(20)	16.90(26)	–	–
124	163	5	540			–	–	–	–	11.80(12)[rec]	–
125	175	–	–			–	–	–	–	–	–
126	171	5	990	09 47 50.69	−21 42 11.71	–	16.63(16)	–	–	–	
127	186	6	540	09 49 24.73	−21 11 11.76	–	17.46(21)	17.28(22)	–	–	–
128	174	6	835.8			–	–	–	–	–	18.5
129	170	1, 2	1080, 972	09 52 26.41	−20 01 07.06	19.51(29)	19.74(54)	–	–	–	–
130	172	1, 3	1080, 2100	09 57 22.17	−21 01 05.40	20.66(16)	20.35(23)	20.02(32)	–	–	–
131	169	5	420	09 51 49.00	−21 33 39.70	16.84(19)	–	–	–	–	
132	167	1, 3	1080, 2100	09 46 02.37	−21 51 44.15	20.24(15)	19.83(20)	19.36(28)	–	–	–
133	183	4	1620	09 51 29.42	−20 25 35.36	19.35(11)	18.87(15)	18.47(16)	17.70(09)	–	–
134	182	1, 2	1080, 2398	09 49 48.77	−21 34 28.21	20.24(15)	20.28(09)	20.36(33)	–		
135	178	1, 2	1080, 2365	09 47 47.91	−21 00 45.22	18.95(13)	18.77(15)	18.71(29)	18.71(38)	–	–
136	181	2	2520	09 54 42.16	−20 49 48.93	20.07(64)	–	–	–	–	–
137	187	5	916.3	09 50 38.70	−21 41 12.24	–	17.24(20)	16.84(22)	16.56(32)	–	–
138	177	6	540	09 55 26.95	−20 46 06.17	–	18.09(19)	17.35(31)	17.07(33)	–	–
139	180	–	–			–	–	–	–	–	–
140	199	5	315	09 45 26.34	−21 55 00.15	–	16.64(20)	16.19(26)	–	–	–
141	189	1, 2	1080, 720	09 45 50.99	−20 14 46.36	19.57(20)	19.29(27)	–	–	–	–
142	195	1, 2	1080, 1793	09 57 15.55	−20 30 34.55	20.43(20)	20.31(25)	–	–	–	–
143	188	1, 2	1080, 724	09 47 46.07	−21 27 50.38	19.59(21)	19.42(38)	–	–	–	–
144	179	6	540	09 49 59.73	−21 27 19.04	–	17.90(26)	17.50(29)	–	–	–
145	137	4	1620	09 48 14.22	−19 59 56.51	17.08(07)	16.60(07)	16.20(08)	15.97(10)	–	–
146	191	–	–			–	–	–	–	–	–
147	197	1	1080	09 45 21.72	−20 35 59.53	18.88(18)	18.62(25)	–	–	–	–
148	162	5	1176			17.54(18)	–	–	–	–	–
149	185	5	990	09 52 14.41	−21 40 18.60	–	14.38(15)	13.95(15)	13.74(16)	–	–
150	194	4	1620	09 45 27.77	−20 57 48.20	14.25(06)	13.88(06)	13.68(06)	13.62(06)	–	–

then it is combined in quadrature with the source counts error (as it already includes the effect of sky variance within an aperture) . If it is negligible, the sky variance within an aperture is used instead.

3 RESULTS

Of the 150 CENSORS sources, 102 likely host galaxy detections were claimed in Paper 1. However, of these two had more than one likely host galaxy candidate; in addition subsequent spectroscopy (see Paper 3) has shown that two candidates were stars and therefore misidentified. Fig. A1 presents the K-band images for those sources for which the K-band data have provided a host galaxy identification, those which remain undetected, and those for which there are complications identifying the host. Some images have been Gaussian-smoothed for clarity. The results of the photometry are given in Table 2. For those sources undetected in K, a 2σ limit based on a 1 arcsec radius aperture is given. Positions based upon the K-band images are given, though it should be noted that for weak detections these may only be accurate to 1 arcsec.

3.1 Using $I - K$ as an indicator of host galaxy type

In the following discussion of individual sources, the $I - K$ colour is used as an indicator that a given galaxy is the correct host galaxy ID. 'Large' values of $I - K$ are used as evidence that a galaxy has an old stellar population. This is based on the fact that radio galaxies are generally hosted by old, giant elliptical galaxies. At any given redshift, these are generally the reddest galaxies because they have the oldest stellar populations. This is demonstrated in Fig. 1 which plots, based upon the K and evolutionary corrections of Poggianti (1997), the predicted $I - K$ for four galaxy types. These galaxy types comprise two elliptical models, E and E2, which differ in their e-folding times for the star formation rate (1 and 1.4 Gyr, respectively) and two spiral models (see Poggianti 1997, for details). At a given redshift the elliptical galaxies always have redder $I - K$ colours, however the actual value of $I - K$ which is considered red varies with the redshift of the galaxy (or the K-band magnitude via the K–z relation). For example, at $z = 0.5$, $I - K = 2.5$ would correspond to a red elliptical, but at $z = 1.5$ such a colour would be typical of a spiral galaxy. Given $I - K$ and an estimate of the redshift this plot can be used to check for consistency with a giant elliptical galaxy, thus giving further evidence that the candidate is, indeed, the host. Note that even redder colours are possible if the star formation time-scale of the ellipticals is shorter. The $I - K$ colours ought to be calculated via I- and K-band magnitudes measured with equal aperture radii. As the EIS I-band photometry was derived using SEXTRACTOR (Bertin & Arnouts 1996), and the K-band magnitude used relatively small aperture radii, the colours obtained give a general, rather than highly accurate, indication of the nature of the host galaxy.

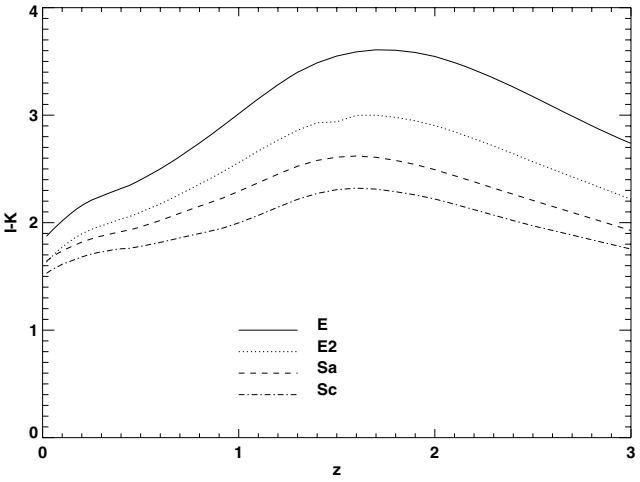

Figure 1. The variation of $I - K$ for four galaxy models as derived from the evolutionary and K-corrections of Poggianti (1997).

3.2 Notes on particular objects

The following are notes regarding particular targets (they include some references to Paper 3).

CENSORS 2: The faint I-band ID is confirmed.

CENSORS 4: The northern of the two I-band candidates has been spectroscopically confirmed as the host galaxy.

CENSORS 7: This faint ID is confirmed in the K band and also spectroscopically.

CENSORS 13: An ID for the host galaxy has been found on the SE component. As discussed in Paper 1, it is likely that the NW radio components are not associated with this and that we have a single source. In that case, those two NW sources do not have sufficient flux to be included in the sample. The radio flux density given for this source, in Paper 1, is for the SE component only.

CENSORS 14: The faint I-band ID is confirmed.

CENSORS 20: There is a potential K-band ID which is a red source associated with the northern radio component. However, spectroscopy (see Paper 3) reveals that emission lines are associated with the centre of the southern component, indicating that the true host is located there. The appropriate magnitude here is then the limiting magnitude at that point, which is 19.4.

CENSORS 28: $I - K \sim 3$. For a low-z galaxy, which must be from its K-band magnitude, this is a very red colour which reinforces this candidate as the likely host galaxy.

CENSORS 31: The western optical source is a star. The eastern candidate has not been spectroscopically confirmed but has $I - K \sim 2.7$ which is not inconsistent with an AGN host at its K–z estimated redshift.

CENSORS 32: The faint I-band ID is confirmed.

CENSORS 37: The faint I-band ID is confirmed in K and also spectroscopically.

CENSORS 38: Whilst this candidate was not found to be likely according to the analysis of Paper 1, subsequent spectroscopy shows that it is a quasar and is therefore the correct identification for the radio source host galaxy.

CENSORS 42: The faint I-band ID is not detected in this (shallow) K-band observation but has a single emission line (see Paper 3) and is therefore correctly identified as the AGN host.

CENSORS 43: The faint I-band ID is confirmed in K and also spectroscopically.

Table 3. Photometry for CENSORS 70. $I - K$ colours are approximate (since no aperture correction has been made) and are based on the 1.5-arcsec aperture.

Candidate	$\sim I - K$
A	3.25
B	2.33
C	>4.1
D	4.07
E	2.14

CENSORS 47: The I-band ID is confirmed in K and also spectroscopically.

CENSORS 57: Whilst no spectroscopic confirmation has been obtained, the red, $I - K \sim 3.7$ colour, of this galaxy provides additional evidence that it is indeed the host galaxy.

CENSORS 58: There is a very tentative detection of a host galaxy for this source, however, a nearby source dominates emission.

CENSORS 60: The I-band ID is confirmed in K and has $I - K \sim 4.5$. This red colour is indicative of a $1 \leqslant z \lesssim 2$ elliptical, consistent with an AGN host.

CENSORS 62: The faint I-band ID is confirmed in K and has $I - K \sim 3$, which is red for its expected redshift.

CENSORS 67: The I-band ID is confirmed in K and has $I - K \sim 2.3$.

CENSORS 69: There is a faint source on the I-band image. However, it was not identified as a likely candidate. There is no detection in the K band so a K-band limit is measured.

CENSORS 70: This is a large extended radio source for which it was not possible to easily associate a host galaxy based on the I-band imaging from EIS. K-band imaging allows candidates to be selected on the basis of colour. These are presented in Table 3. Since CENSORS 70 is a fairly large radio source (3 arcmin) it is likely that it is at relatively low redshifts (at $z > 1$ this angular size corresponds to $\sim$1 Mpc). Thus candidates B and E, which have $I - K$ typical of elliptical galaxies at $z < 1$, are, by this argument, the most likely candidates. This issue is unlikely to be resolved without spectroscopic follow-up of all these candidates.

CENSORS 74: There were no likely candidates according to the analysis of Paper 1; however, there are two optical sources visible in the I-band image which might be associated with radio source. K-band imaging reveals that the more eastern of these two is a mildly red ($I - K \sim 2.9$) source and is adopted as the candidate.

CENSORS 81: The host galaxy is detected in K and has been spectroscopically confirmed.

CENSORS 82: The identification came from the I band, but the spectrum shows this to be a star. There is no host galaxy candidate from the K band.

CENSORS 84: As discussed in Paper 1 this radio source (EISD 103) was associated with EISD 73 and 151. It is believed that EISD 73 and 151 were correlated noise in the NVSS data thus leaving EISD 103. The higher-resolution maps then revealed this to be two radio sources leaving the possibility that either they were associated, and would therefore have sufficient combined flux to be included in CENSORS, or that they were unassociated. The K-band imaging reveals that there is no red galaxy between the two radio sources that might indicate that they are associated and are radio lobes. There is a candidate host galaxy associated with the western radio source. This is taken to be the correct host galaxy for this source and it continues

to be included in the CENSORS sample on the assumption that the eastern source is associated with it.

CENSORS 86: The host galaxy is detected in K and, whilst not spectroscopically confirmed, $I - K = 5.3$ and this is typical of the old elliptical galaxies which host AGN.

CENSORS 89: There are two K-band candidates for this source. The eastern identification emits an [O II] line and shows strong H and K absorption features (see Paper 3).

CENSORS 90: As discussed in Paper 1, CENSORS 90 and 103 (EISD 114 and 56, respectively) may be associated (CENSORS 10/EISD 16 is nearby but is clearly associated with a double radio source). Fig. A2 shows the I- and K-band images with the radio contours. Component A is CENSORS 10. It was suggested that the optical counterpart to component F was evidence that it was a single source, too weak to be included in the CENSORS sample. This is consistent with the counterpart being a red source, detected in the K band. B may correspond to CENSORS 90 while component E corresponds to CENSORS 103; component D has a counterpart and causes the NVSS map for CENSORS 103 to be extended to the NE. However, neither component B nor E has a counterpart in either the optical or near-IR, whereas component C does and lie between the two, raising the possibility that B, C and E are associated.

CENSORS 94: The off-axis NE source is believed to be the host galaxy. The other candidate is a star and the NE source has $I - K > 4$.

CENSORS 97: $I - K \sim 3.2$ confirms this as the likely candidate.

CENSORS 103: See CENSORS 90.

CENSORS 104: There is no spectroscopic confirmation but this has $I - K \sim 5.3$.

CENSORS 105: This red ($I - K \gtrsim 3.3$) host galaxy candidate is confirmed by extended Lyα emission (Paper 3).

CENSORS 107: This galaxy has $I - K \gtrsim 2.6$, and has been shown spectroscopically to be at $z \sim 0.5$ (Paper 3). The spectrum is of an old galaxy, and the colour is red for that redshift, suggesting that this is indeed the host.

CENSORS 109: With $I - K \gtrsim 2.9$, this is a relatively red galaxy for its expected redshift.

CENSORS 115: This galaxy has $I - K \gtrsim 2.6$. Again the spectrum shows a well-defined 4000-Å break and G-band absorption. This indicates that the galaxy is old and therefore a reasonable identification for the host.

CENSORS 126: There were two I-band identifications for this object one of which has been identified as a star via spectroscopy. The second candidate is taken as the host galaxy; however, the radio emission does not clearly associate with this optical/near-IR source by eye. The second candidate is apparently unresolved in the K-band image; however, it is very close to the star making it difficult to tell. It is possible that the true ID could be hidden behind the star.

CENSORS 133: The red colour, $I - K \gtrsim 4$, of this galaxy, in addition to its position, coincident with the radio source, makes it the likely host.

CENSORS 135: The candidate found on one component is confirmed in the K band. It has a colour of $I - K \gtrsim 2.5$, which is potentially blue.

CENSORS 136: A red source appears in the K band. It is somewhat offset from the main radio component, but may be reasonable if the radio emission to the south of the main component is associated with this source.

CENSORS 148: This host galaxy is very close to a brighter nearby object. This means that the quoted error on the magnitude may be optimistic.

CENSORS 150: There is no clear candidate associated with the source. For now the brightest galaxy is taken to be the host galaxy.

3.3 Summary

142 of the 150 CENSORS sources have been targeted in the K band. There are 18 sources for which a host galaxy is not clearly detected. However, of these, six are detected in the I band. The remaining 12 are CENSORS 20, 26, 58, 64, 69, 70, 82, 85, 87, 90, 103 and 150. Some of these sources have complications, for example, as discussed in Paper 1, CENSORS 82 may be associated with CENSORS 66 (which has an I-band identification) and CENSORS 90 may be associated with CENSORS 103. Whilst CENSORS 20 has no identified host galaxy, a spectrum taken at the radio source position shows two emission lines ($z = 1.38$). CENSORS 85 has no clear host galaxy identification but this may be due to the complexity of the radio map rather than lack of depth in the optical and IR images. CENSORS 58 is very close to a bright star, making it very difficult to detect the host; CENSORS 150 has no obvious candidate host and CENSORS 70 has several candidates (though spectroscopic targeting ought to resolve the correct host). Low-frequency radio data, which has recently been obtained at 610 and 325 MHz, may help to resolve issues where interpretation of the radio data is difficult. This leaves four sources which are not detected and have no other complications: these are likely to be cases of high-redshift host galaxies, and deeper IR images are required.

There may also be, as yet unidentified, problems due to lensing of radio sources. It may be possible that a radio source has been associated with a relatively low-redshift galaxy (and subsequently its redshift) when in fact the low-redshift galaxy is lensing the radio source which is actually at a high redshift. This could have consequences when the redshifts ascribed to radio sources are used in the modelling of the radio luminosity function.

4 APERTURE CORRECTIONS

Of the 142 CENSORS sources which are imaged in the K band, 78 are detected and have spectroscopic redshifts (which are presented in Paper 3). Using these redshifts, the observed K-band magnitude may be corrected to a consistent, physical radius thus allowing direct comparison of the magnitudes of the sources.

The K-band magnitudes presented here were measured in aperture of radii 1, 1.5, 2.5 and 4.5 arcsec. Ideally a very large aperture would be used in order to be sensitive to the whole galaxy. However, the level of the sky background will affect the maximum-radius aperture that is possible. In order to compare the magnitudes of galaxies, the magnitudes are corrected to an aperture of 63.9 kpc (chosen for consistency with previous work). Since most low-redshift radio galaxies reside in large elliptical galaxies, the emission from the host galaxies will follow a curve of growth which can be used to correct the magnitudes. The curve of growth presented in Sandage (1972) has been used to correct galaxies with redshift $z < 0.6$. High-redshift galaxies do not always have the same structures as those at low redshift so this method is not appropriate for them and so, following Eales et al. (1997), it is assumed that emission from higher-redshift galaxies, measured within an aperture of radius, r, is proportional to r^{α}, where $\alpha = 0.35$.

Where there was a choice of aperture, corrections were calculated for all. The corrected magnitude with the least error (including an estimated 15 per cent error on the correction term, in order to account for an uncertainty in making the correction) was used. This also allowed a check that aperture corrections agreed for different

Table 4. Aperture-corrected K-band magnitudes for all sources with a measured spectroscopic redshift (presented in Paper 3) and a K-band detection. Columns list the CENSORS and EIS identifiers; the redshifts; the aperture radius used to measure the K-band magnitude; the measured aperture magnitude; the magnitude after correction to 63.9 kpc; the error on the corrected magnitude (in units of 0.01 mag) and the classification of the sources as radio galaxies (G), quasars (Q) or star forming galaxies(S). Paper 3 discusses the evidence upon which these classifications are made.

CENSORS	EIS	z	θ_m (arcsec)	K (θ_m)	K (63.9 kpc)	δK	Class
1	1	1.1550	1.5	18.13	17.78	30	G
2	2	0.9130	1.0	19.00	18.47	19	G
3	3	0.7900	2.5	16.67	16.47	15	G
4	6	1.0130	2.5	17.82	17.65	27	G
5	8	1.5880	1.5	19.35	19.01	34	G
6	7	0.5470	2.5	16.18	16.18	16	Q
7	10	1.4370	2.5	17.79	17.79	33	Q
9	12	0.2420	2.5	16.30	15.74	25	G
10	16	1.0740	2.5	15.98	15.98	7	Q
12	18	0.8210	1.5	19.13	18.74	31	G
13	20	2.9500	1.5	19.86	19.49	21	G
16	23	3.1260	1.0	19.85	19.32	41	G
17	24	0.8930	2.5	18.02	17.84	30	G
18	25	0.1090	4.5	13.02	12.45	23	G
24	32	3.4310	1.5	19.69	19.30	31	G
27	44	0.4230	4.5	15.87	15.78	23	G
28	38	0.4720	4.5	15.98	15.91	11	G
29	39	0.9650	2.5	17.29	17.29	23	Q
32	43	1.1510	1.5	17.91	17.56	23	G
33	45	1.2030	2.5	18.91	18.75	27	G
35	48	0.4730	4.5	16.53	16.46	20	G
37	52	0.5110	1.5	19.45	19.45	26	Q
38	53	2.1160	2.5	17.25	17.25	15	Q
39	54	1.5720	2.5	17.63	17.63	33	Q
41	58	0.2950	4.5	15.07	14.89	21	G
43	64	0.7780	1.5	17.54	17.15	24	G
44	62	0.7900	2.5	17.98	17.98	30	Q
45	66	0.7960	2.5	17.04	16.84	13	G
46	65	0.7180	2.5	17.15	16.94	13	G
47	63	0.5080	4.5	16.50	16.45	21	G
49	67	0.4100	4.5	15.88	15.78	25	G
52	72	1.6245	1.0	18.93	18.43	22	G
53	76	0.4260	2.5	15.60	15.24	22	G
54	74	0.4100	4.5	14.25	14.15	11	G
55	71	0.5570	4.5	16.67	16.64	15	G
62	84	0.5740	1.5	17.41	16.81	28	G
63	88	0.3020	4.5	16.25	16.08	25	G
65	87	0.5490	2.5	16.95	16.65	26	G
67	89	0.4280	4.5	16.05	15.96	18	G
68	91	0.5140	1.5	16.91	16.28	22	G
72	97	2.4270	2.5	18.04	17.88	21	G
75	98	0.2650	2.5	15.32	14.80	20	G
76	102	0.2820	4.5	15.28	15.09	31	G
77	104	1.5120	1.5	19.01	18.67	30	G
79	106	1.2550	4.5	17.37	17.44	25	G
80	110	0.3660	4.5	14.77	14.65	15	G
83	116	0.5210	2.5	16.48	16.17	22	G
89	117	0.9090	1.5	19.53	19.16	32	G
92	122	0.7430	2.5	16.47	16.47	25	Q
93	132	0.1830	1.5	16.21	15.13	31	G
95	123	0.0450	4.5	13.25	12.08	27	S
96	131	2.7060	1.0	20.59	20.07	27	G
99	133	0.7380	4.5	16.18	16.20	21	G
102	134	0.4680	2.5	15.97	15.63	28	G
105	138	3.3770	1.0	20.70	20.16	36	G
107	148	0.5120	2.5	16.32	16.01	17	G
108	153	0.2300	4.5	14.93	14.68	23	G
111	149	0.4110	4.5	15.94	15.84	24	G
114	166	1.4260	1.5	19.23	19.23	34	Q
115	155	0.5450	4.5	15.22	15.18	23	G
116	143	2.6370	2.5	18.23	18.23	27	Q
117	165	1.2040	2.5	18.31	18.15	33	G
118	161	2.2940	1.0	19.82	19.31	22	G
120	159	2.8290	1.5	17.68	17.31	24	G
121	164	0.2460	4.5	14.86	14.64	20	G
122	156	0.2500	4.5	14.62	14.40	22	G
127	186	0.9220	2.5	17.28	17.10	24	G
129	170	2.4210	1.0	19.51	19.00	36	G
131	169	0.4700	1.0	16.84	15.87	33	G
134	182	2.3540	1.5	20.28	19.93	14	G
137	187	0.5260	2.5	16.84	16.53	26	G
138	177	0.5080	2.5	17.35	17.03	35	G
140	199	0.2650	2.5	16.19	15.67	33	G
141	189	2.8290	1.0	19.57	19.05	27	G
144	179	0.6960	2.5	17.50	17.28	32	G
145	137	0.4000	4.5	15.97	15.87	11	G
149	185	0.0290	2.5	13.95	12.58	35	S

aperture sizes, within the errors. Aperture sizes below 2.5 arcsec have only been used when either a contaminating galaxy is present, or the radio galaxy is so faint that larger apertures give photometric errors in excess of 0.35 mag. No corrections are applied for quasar K-band magnitudes, as they are point-like sources.

The corrected K-band magnitudes are presented in Table 4. This table also lists the quasars and star forming galaxies that are identified in Paper 3.

5 THE CENSORS K–z RELATION

As described in Section 1, the K–z relation is known to vary for radio-selected samples of different flux-density limit. Previous work with the 3CRR, 6C and 7C surveys has shown that whilst the 6C and 3CRR samples share a similar K–z relation at low redshifts, the 6C sample, which is around five times fainter than 3CRR, is 0.6 mag fainter at $z > 1$ (see, for example, Lilly & Longair 1984; Eales & Rawlings 1996; Inskip et al. 2002). Willott et al. (2003) showed that the 7C sample (which is a further four times fainter in radio flux-density limit than 6C) is fainter in the K-band than 3CRR at all redshifts and speculates that the 6C sample, which is sparse in objects at the lowest redshifts, and therefore carries a large error, may be consistent with being fainter in K at low redshifts too.

The spectroscopic completeness of the CENSORS sample is 60 per cent, and so it is possible to make a comparison of the CENSORS K–z relation against the previous work. This is done whilst noting that strong conclusions should be delayed until the spectroscopic completeness is higher.

Fig. 2 plots the aperture-corrected K-band magnitude against redshift for all sources for which both these variables have been measured; excluding two star forming galaxies (CENSORS 95 and 149) and 11 quasars (CENSORS 6, 7, 10, 29, 37, 38, 39, 44, 92, 114 and 116) as these will be hosted by different galaxies. The identification of the quasars and star forming galaxies is largely based upon spectroscopic evidence and is discussed in full detail in Paper 3. Overplotted are the K–z relations from: Willott et al. (2003) (solid

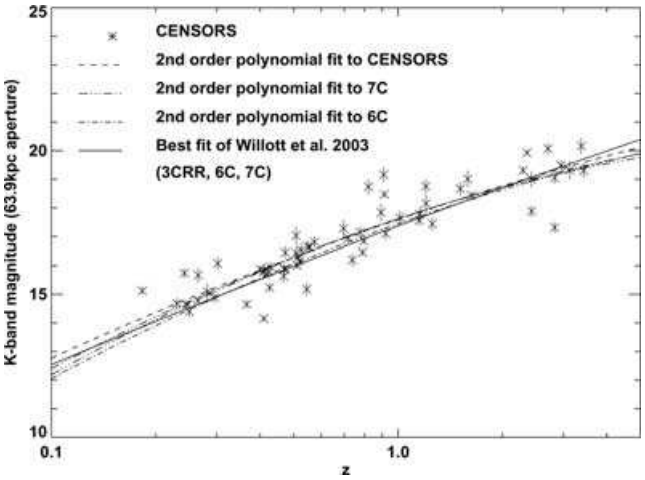

Figure 2. *K*-band magnitude against redshift for all CENSORS sources for which both are available, excluding star forming galaxies and quasars. The solid line shows the best-fitting relation of Willott et al. (2003) which is a second-order polynomial in log z, derived using the 3CRR, 6CE, 6C* and 7C regions I, II and III. The dot–dash line shows the K–z relation as derived for the 6C samples used by Willott et al. (2003) and the dash–triple dot line shows that of the 7C samples used by Willott et al. (2003). The dashed line is the best-fitting relation based upon the CENSORS sample alone. The 6C, 7C and CENSORS fits are also polynomials of second order in log z.

line, based upon 3CRR, 6C and 7C); the K–z relation based upon the 6CE and 6C* samples alone (dash–dot); the 7C sample (regions I, II and III) alone (dash–triple dot) and the CENSORS points (dashed). All fits are second-order polynomials in log z and the 6C and 7C samples used are identical to those used in Willott et al. (2003).

The Willott fit is clearly a reasonable fit to the CENSORS; however, the CENSORS best fit is fainter at low redshifts. The 7C fit is given by

$$K = 17.62 + 4.04 \log z - 1.39 \log^2 z, \quad (1)$$

and shows that in fact the CENSORS sample is in better agreement with the 7C sample rather than the 3CRR. Note that no fit to the CENSORS data points is given due to the incomplete spectroscopic information for this sample at present. These low-redshift differences are investigated in Fig. 3(a) which plots the difference between the CENSORS sample and the best-fitting K–z relation of Willott et al. (2003). This figure replicates fig. 3 of Willott et al. (2003) but uses bins of width $z = 0.62$, rather than 0.6, plotted in steps of $\Delta z = 0.2$. The change in bin size ensures that every bin has more than one source. The errors bars show the standard errors and are correlated as a result of the overlapping bins. This figure shows that CENSORS is fainter than 3CRR over all redshifts and by a similar magnitude as the 7C sample. At redshifts greater than $\sim$2 there appears to be little difference between the CENSORS points and the best fit. However, at these redshifts there are no 3CRR sources and so the best fit is essentially a fit to the 6C and 7C samples alone. This is further demonstrated in Fig. 3(b) which plots the K-band offsets of the CENSORS sources from the 7C K–z relation.

This indicates that it is the 3CRR K–z relation that should be considered 'anomalous' as the other surveys tend to agree with a more consistent relation. The simplest interpretation of this would be that the most powerful radio sources, as sampled by the 3CRR sample, have additional K-band light either directly or indirectly associated with the AGN activity (e.g. through associated star formation). However, at lowest redshifts, the 3CRR sources are not believed to be

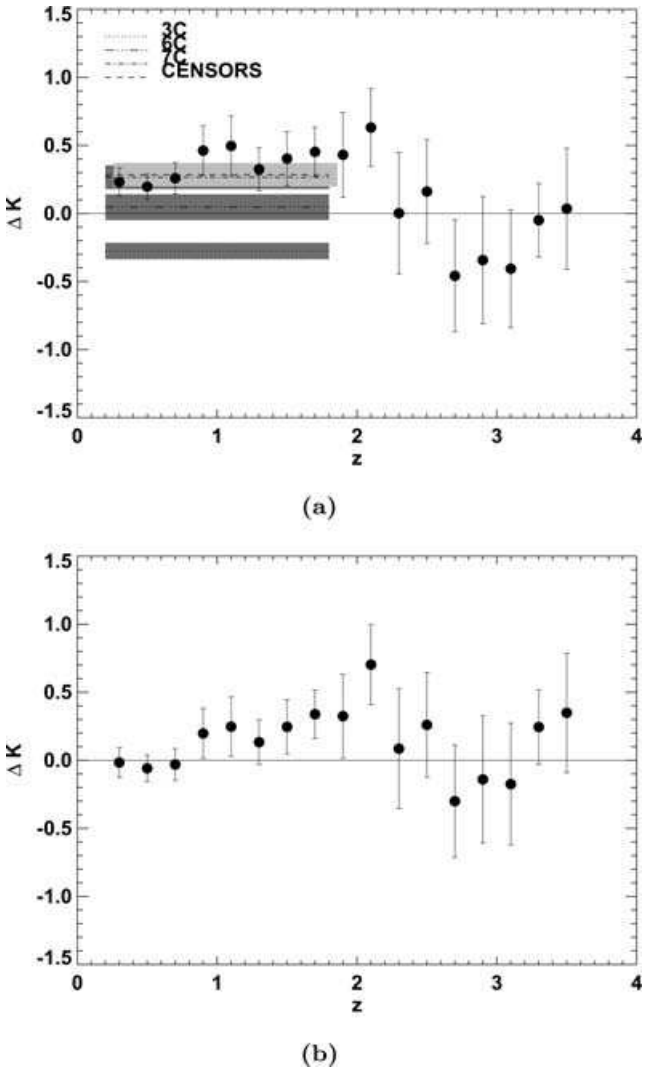

Figure 3. (a) The offset, ΔK, of the CENSORS sources (where both a K-band magnitude and spectroscopic redshift are available, and excluding star forming sources and quasars) compared to the best-fitting K–z relation for radio galaxies from Willott et al. (2003) (based upon 3CRR, 6CE, 6C* and 7C, I, II and II). Here $\Delta K = K - K_{\rm fit}$. Overplotted are the mean ΔK values for the 3CRR (dotted), 6C (dash–triple dot), 7C(dash–dot) and CENSORS (dashed) in the range $0.2 < z < 1.8$. The shaded regions indicate the 1σ standard errors about the means and the shaded region for the CENSORS sample has been offset 0.06 in z in order that the extent of the 7C standard errors may be displayed. This plot is based upon fig. 3 of Willott et al. (2003) and the relevant data were provided by Willott (private communication). The data are investigated in bins of width $z = 0.62$ plotted in steps of $\Delta z = 0.2$. The error bars show the standard errors and are correlated as a result of the overlapping bins. (b) K-band offsets of the CENSORS sources as compared to the K–z relation based upon 7C only.

significantly AGN contaminated (e.g. Best et al. 1998). So, it may be wiser to consider these data as a constraint on the link between K-band magnitude and radio luminosity, via galaxy mass and black hole mass, given variations in the accretion rate. These conclusions however are made with only 60 per cent spectroscopic completeness in the CENSORS sample and so a full analysis must be left until that figure has increased. At $z < 1$, redshifts are obtained from emission lines or features in bright continua; therefore, the spectroscopically identified sources may be biased to be brighter objects. However,

at these redshifts our spectroscopic completeness is believed to be quite high ($\geqslant$80 per cent, see Paper 3). Higher-redshift objects tend to be spectroscopically identified by emission lines alone and so may be less biased to bright galaxies, though they will still suffer bias due to secondary effects.

Despite these difficulties, given that our spectroscopic completeness is likely to be higher at low redshifts than at high redshifts, the result that CENSORS is fainter in the K-band than 3CRR and of similar magnitude to 7C seems likely to stand upon further investigation. In the meantime, it is sufficient to conclude that the CENSORS K–z relation is not substantially different from the best fit to the 7C data and that relation may be used to estimate redshifts for the non-spectroscopically identified CENSORS host galaxies.

6 SUMMARY

Of the 150 CENSORS sources, 142 have been observed in the K band using the AAT, UKIRT and the VLT over the last 3 yr. These images have been used to identify the host galaxies of CENSORS sources which lack an identification in the EIS I-band images and to provide K-band photometry for all CENSORS sources, where possible.

Of the eight sources not observed in the K band, seven have I-band identifications of the radio source host galaxy and the remaining source has a weak I-band detection, which, when targeted spectroscopically, yielded a single emission line (see Paper 3).

There are 18 sources for which a host galaxy is not clearly detected. However, of these, six are detected in the I band. Of the remaining 12 some have complications, such as possible association with other radio sources or numerous outstanding candidate host galaxies, leading to uncertainty. Low-frequency radio data, obtained at 610 and 325 MHz, may help to resolve issues where interpretation of the radio data is difficult. Four sources that remain undetected are likely to be cases of high-redshift host galaxies, and deeper IR images are required.

Aperture corrections have been calculated for those sources with a K-band magnitude presented in this paper and a spectroscopic redshift presented in Paper 3. From these a K–z relationship for the radio galaxies of the CENSORS sample has been established and shown to be offset to fainter K-band magnitudes over the range $0.2 < z < 1.8$ with respect to the best-fitting K–z relation of Willott et al. (2003). Since the K-band magnitudes of 3CRR sources (at low redshift) are not believed to be significantly affected by the AGN, this provides constraints on any model which attempts to explain the K–z relation in terms of black hole mass and accretion rate. However, these conclusions should be taken on the understanding that a higher spectroscopic completeness, in the CENSORS sample, is required before it is considered certain.

ACKNOWLEDGMENTS

MHB is grateful for the support of a PPARC research studentship. Observations were made using the United Kingdom Infrared Telescope which is operated by the Joint Astronomy Centre on behalf of the UK Particle Physics and Astronomy Research Council. Further observations were carried out using the Anglo-Australian Telescope and the ESO VLT at the Paranal observatory (Program ID number 69.A-0047).

REFERENCES

Bertin E., Arnouts S., 1996, A&AS, 117, 393
Best P. N., 2000, MNRAS, 317, 720
Best P. N., Longair M. S., Röttgering H. J. A., 1998, MNRAS, 295, 549
Best P. N., Arts J. N., Röttgering H. J. A., Rengelink R., Brookes M. H., Wall J., 2003, MNRAS, 346, 627 (Paper 1)
Blundell K. M., Rawlings S., Eales S. A., Taylor G. B., Bradley A. D., 1998, MNRAS, 295, 265
Casali M. M., Hawarden T. G., 1992, UKIRT Newslett., 4, 33
Condon J. J., Cotton W. D., Greisen E. W., Yin Q. F., Perley R. A., Taylor G. B., Broderick J. J., 1998, AJ, 115, 1693
Eales S., Rawlings S., Law-Green D., Cotter G., Lacy M., 1997, MNRAS, 291, 593
Eales S. A., Rawlings S., 1996, ApJ, 460, 68
Fanaroff B. L., Riley J. M., 1974, MNRAS, 167, 31P
Eales S. A., 1985, MNRAS, 217, 149
Inskip K. J., Best P. N., Longair M. S., MacKay D. J. C., 2002, MNRAS, 329, 277
Jarvis M. J., Rawlings S., Eales S., Blundell K. M., Bunker A. J., Croft S., McLure R. J., Willott C. J., 2001, MNRAS, 326, 1585
Kormendy J., Gebhardt K., 2001, in AIP Conf. Proc., Vol. 586, 20th Texas Symposium on Relativistic Astrophysics Supermassive Black Holes in Galactic Nuclei (Plenary Talk). Am. Inst. Phys., New York, p. 363
Lilly S. J., Longair M. S., 1984, MNRAS, 211, 833
Nonino M. et al., 1999, A&AS, 137, 51
Poggianti B. M., 1997, A&AS, 122, 399
Sandage A., 1972, ApJ, 173, 485
Tody D., 1986, in Instrumentation in Astronomy VI, Proc. Meeting, Tucson, AZ. Society of Photo-Optical Instrumentation Engineers. p. 733
Tody D., 1993, in ASP Conf. Ser., Vol. 52, Astronomical Data Analysis Software and Systems II IRAF in the Nineties. Astron. Soc. Pac., San Francisco, p. 173
Willott C. J., Rawlings S., Jarvis M. J., Blundell K. M., 2003, MNRAS, 339, 173

APPENDIX A: *K*-BAND IMAGES OF CENSORS SOURCES

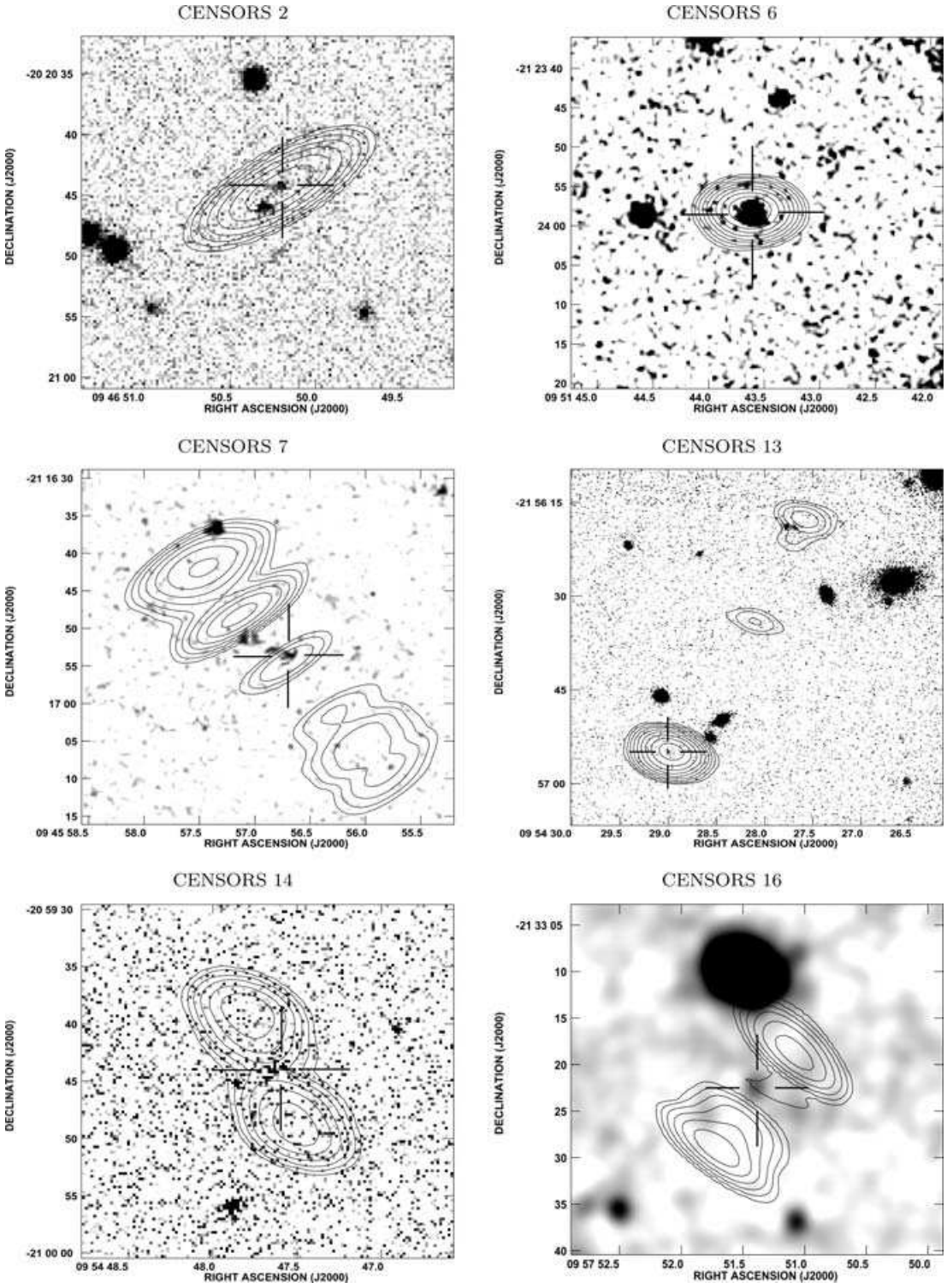

Figure A1. CENSORS *K*-band images are shown in grey-scale. Some images have been Gaussian-smoothed for clarity. The contours plot the radio maps (presented in Paper 1) based upon VLA observations in BnA and CnB array at 1.4 GHz. The resolution of the radio maps is 7 arcsec or better, and in many cases reaches 3 or 4 arcsec (see Paper 1 for details).

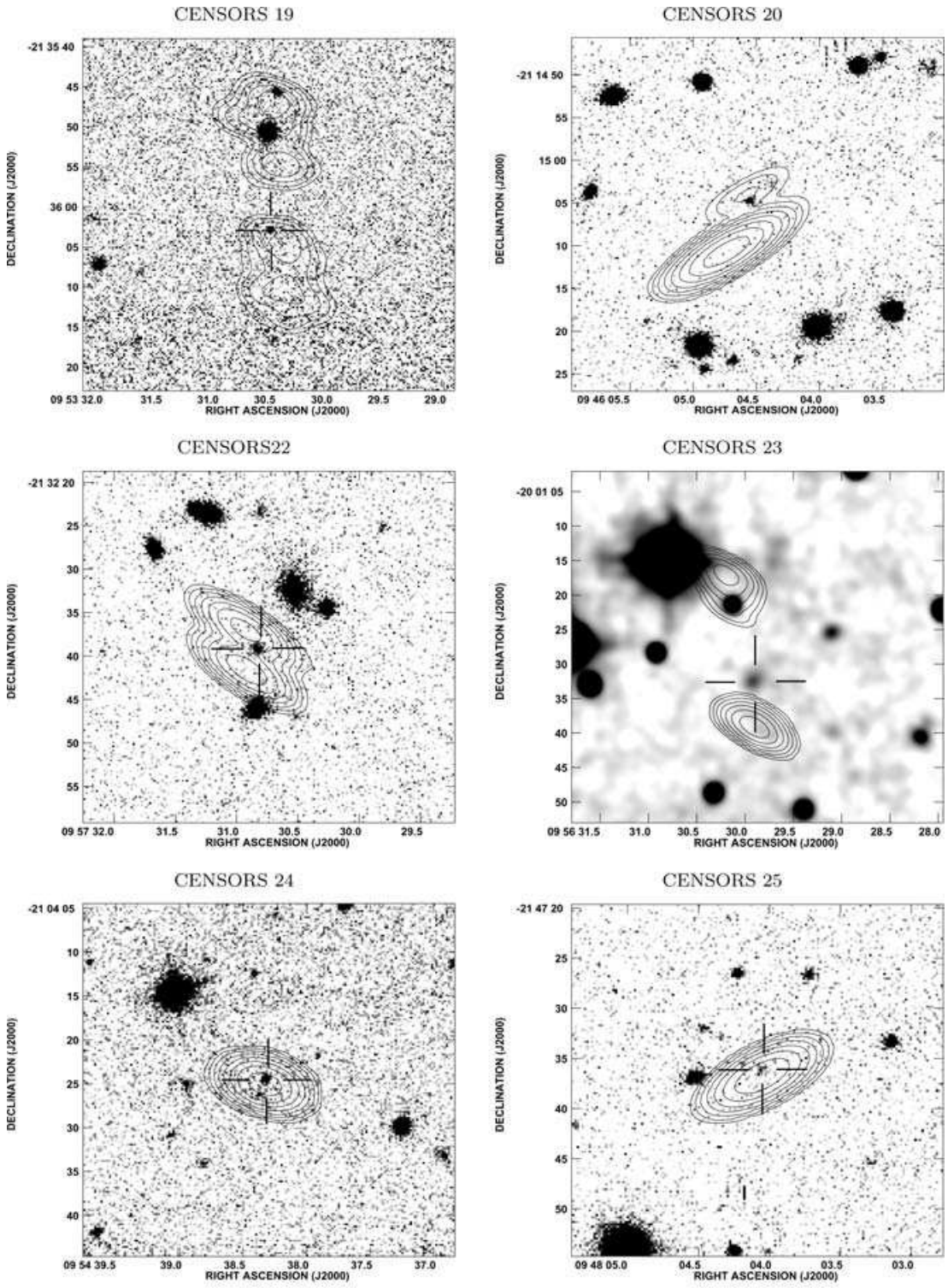

Figure A1 – *continued*

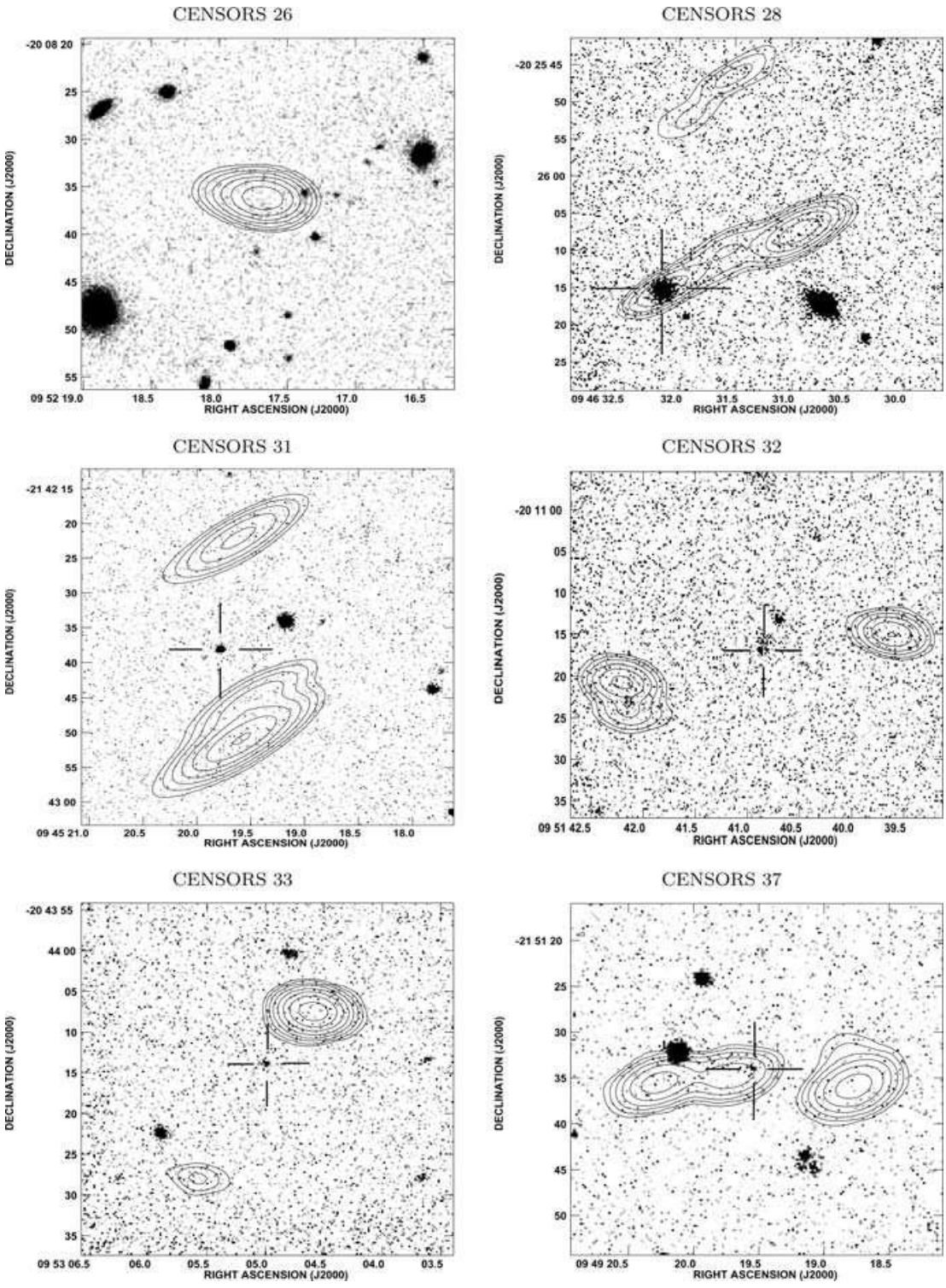

Figure A1 – *continued*

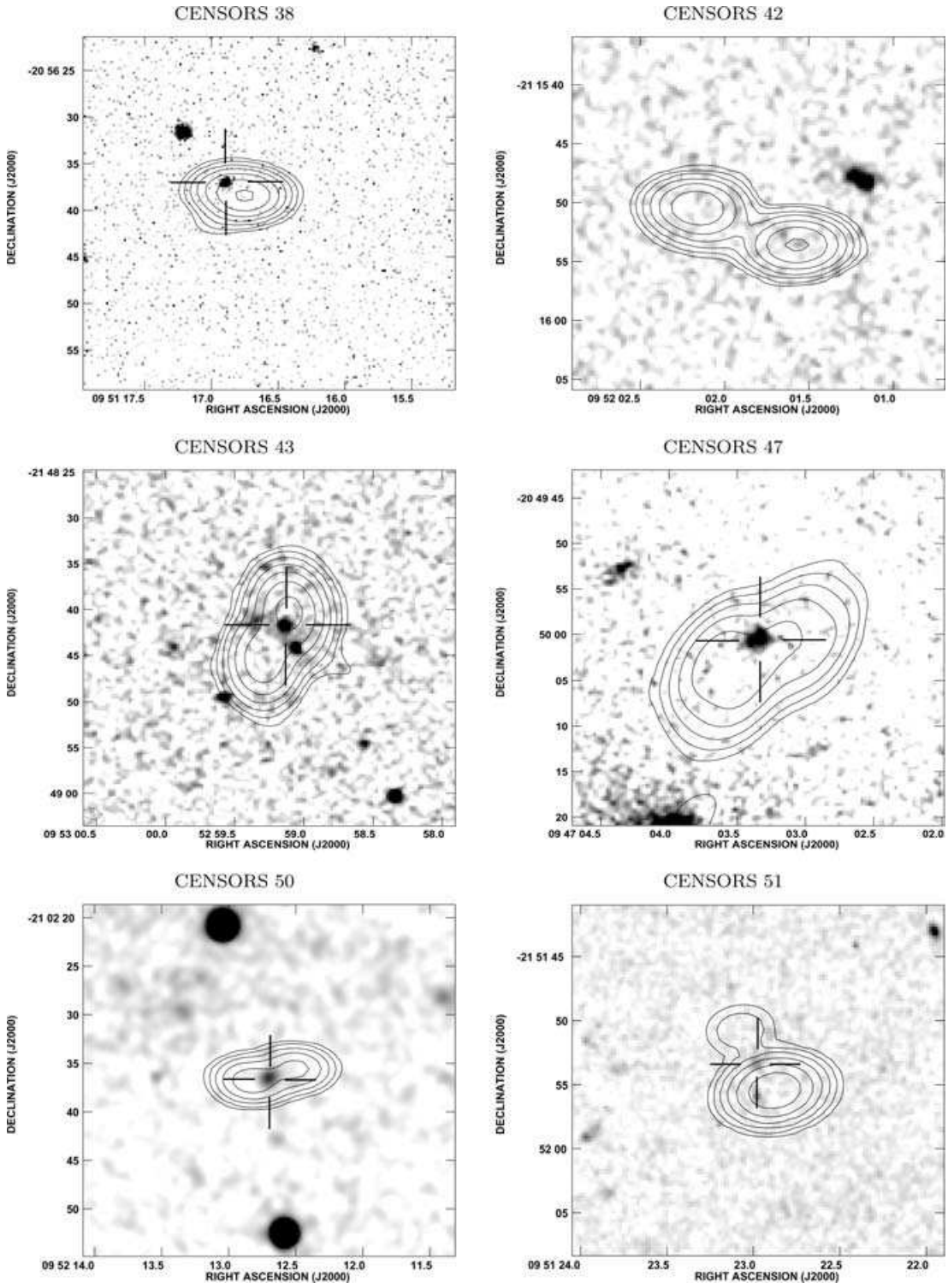

Figure A1 – *continued*

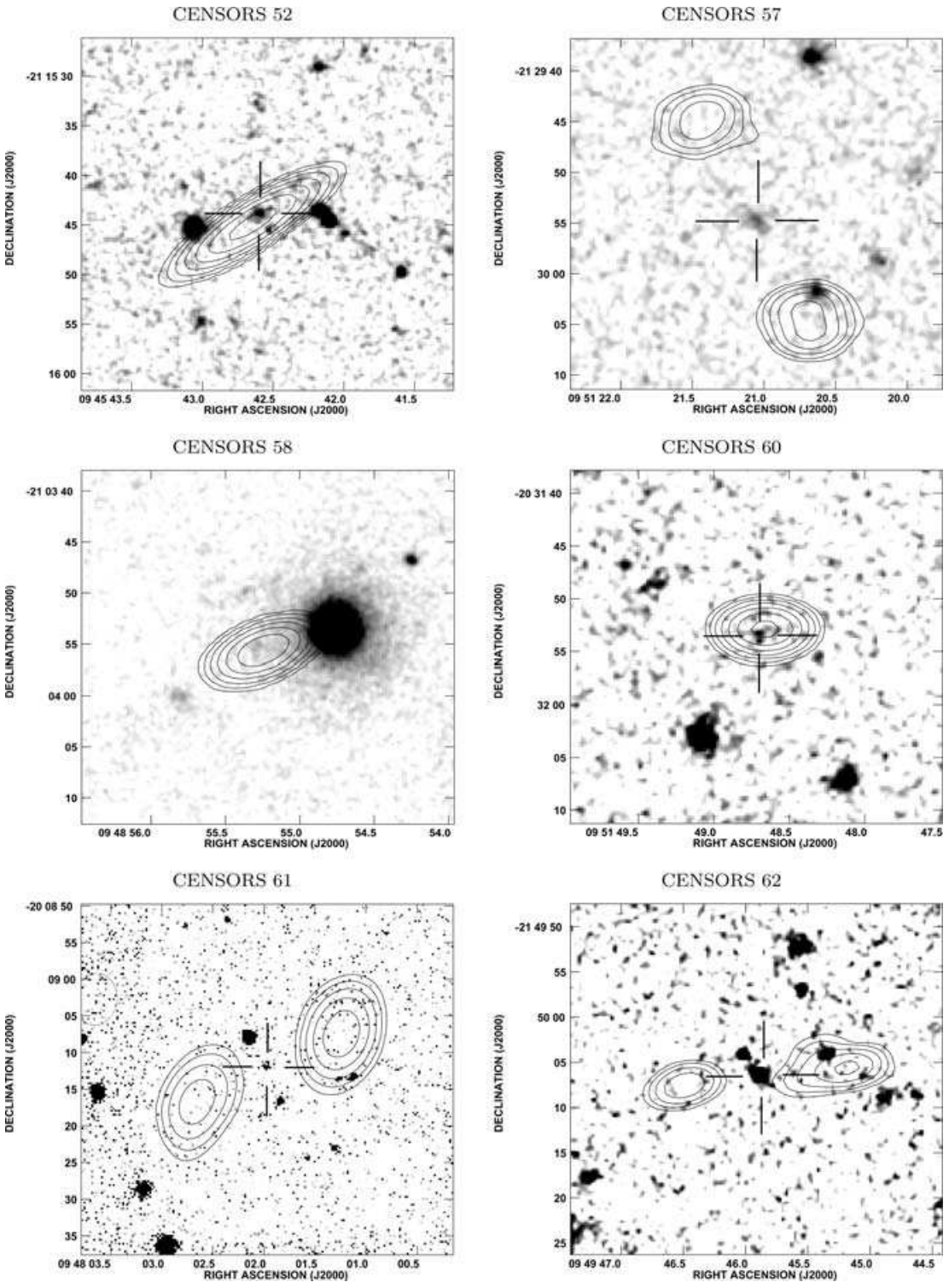

Figure A1 – *continued*

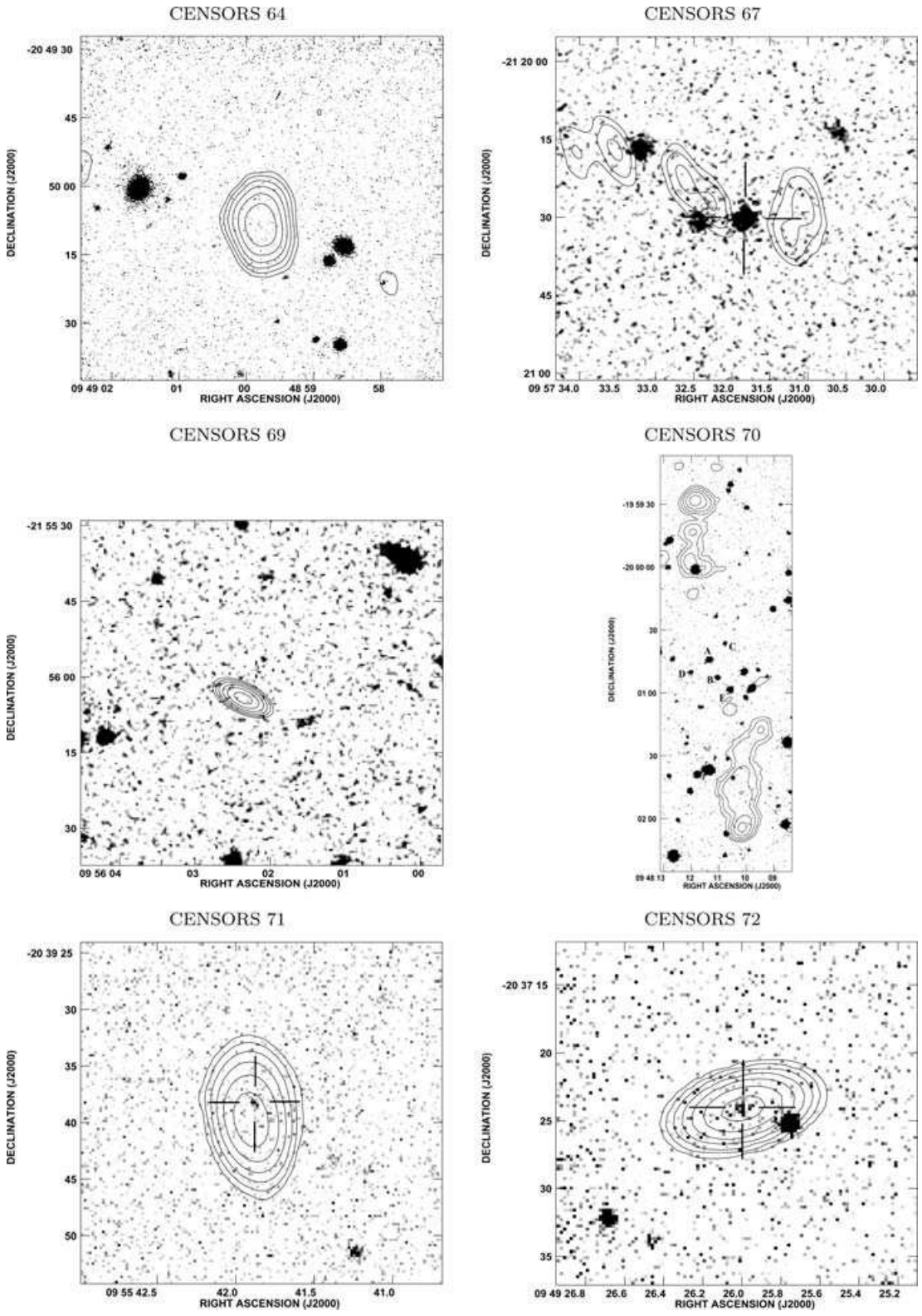

Figure A1 – *continued*

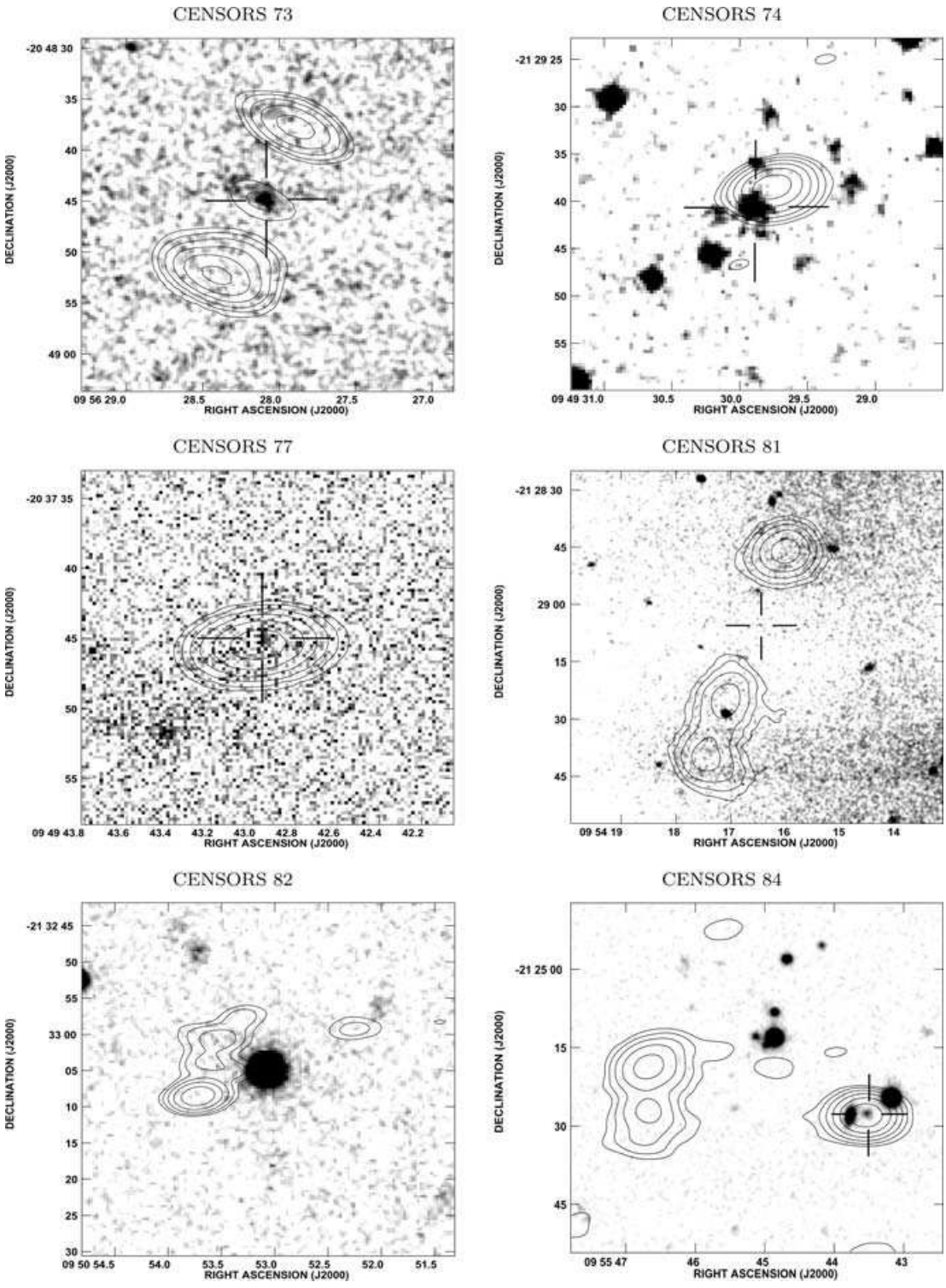

Figure A1 – *continued*

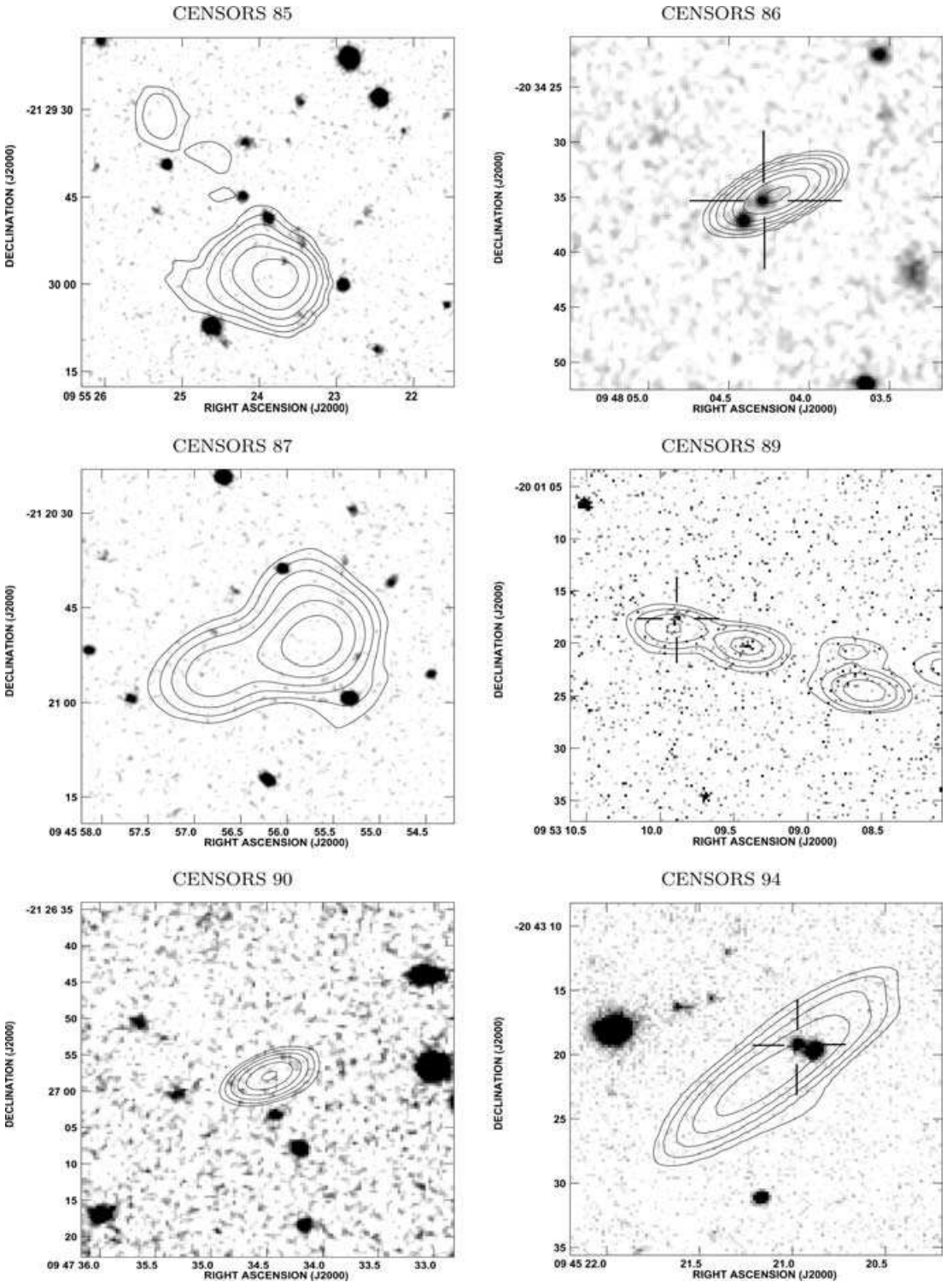

Figure A1 – *continued*

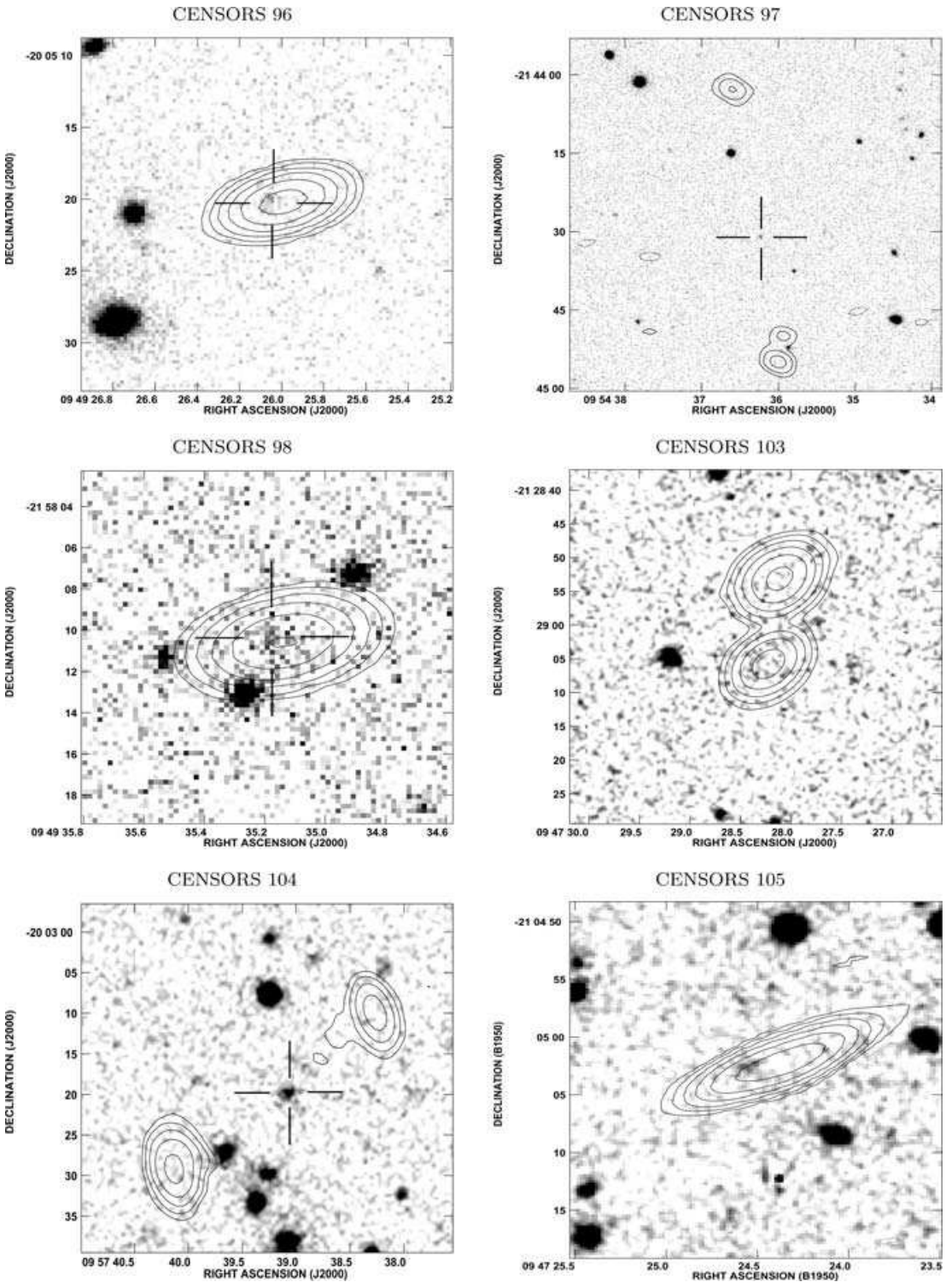

Figure A1 – *continued*

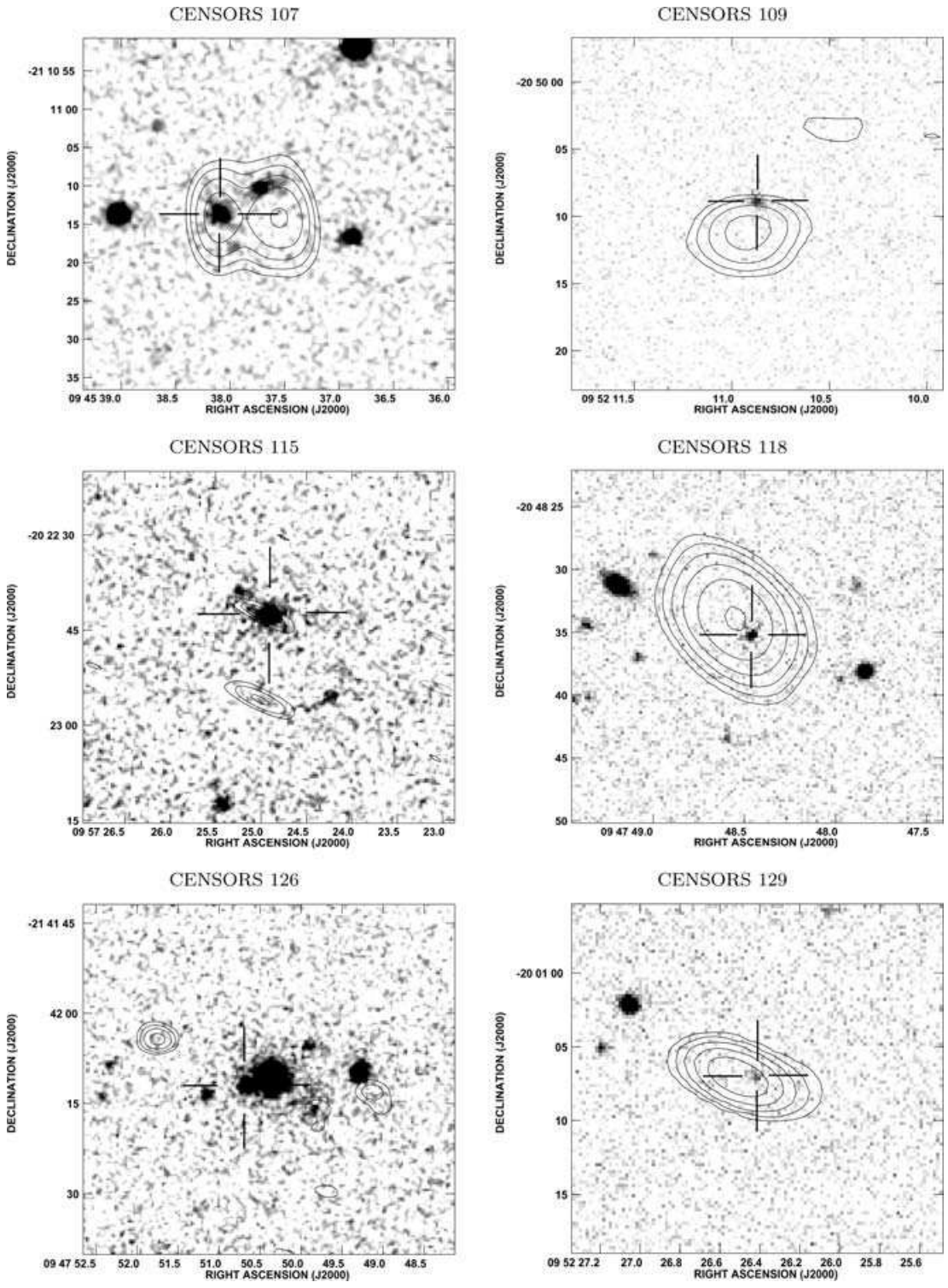

Figure A1 – *continued*

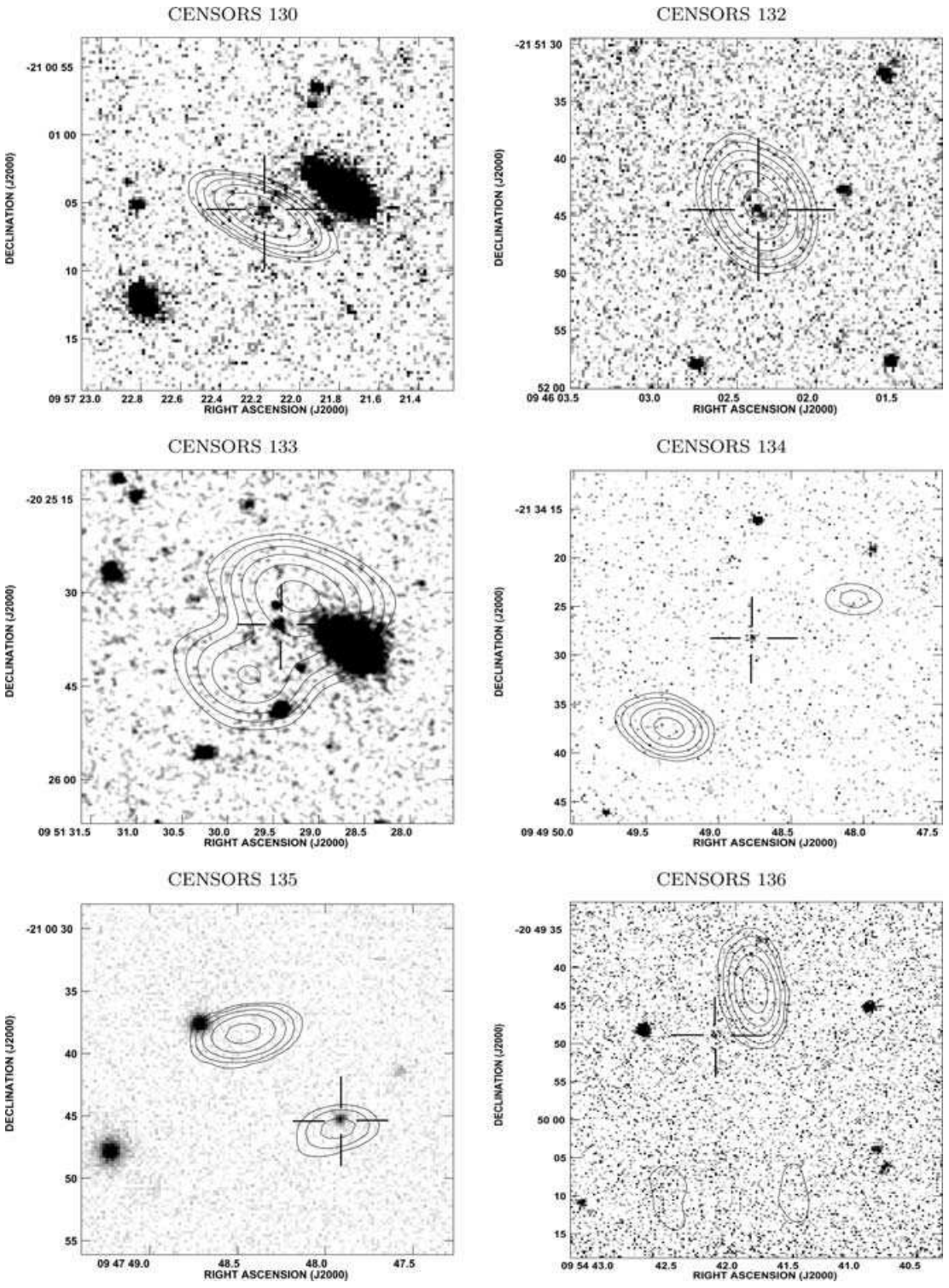

Figure A1 – *continued*

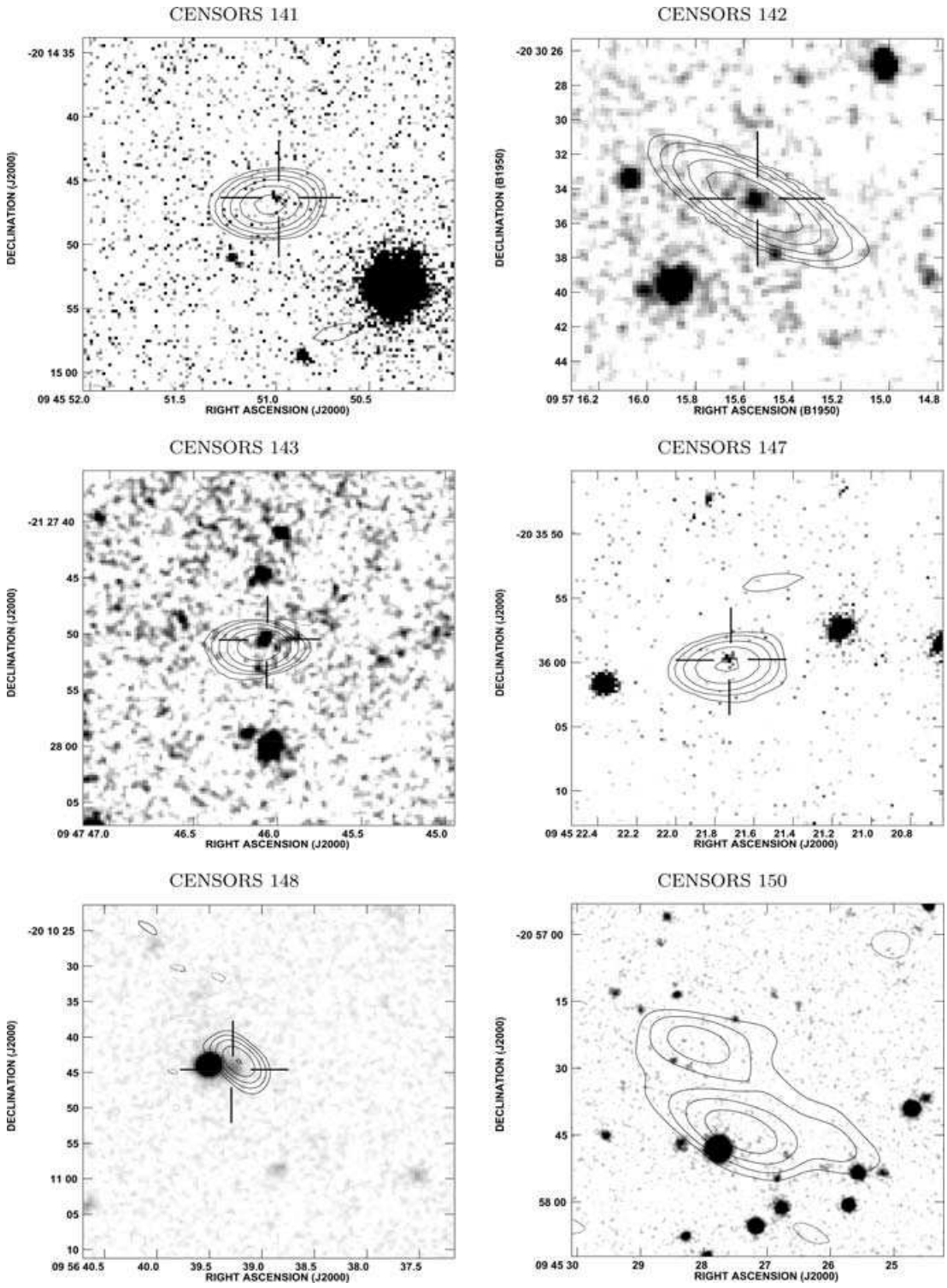

Figure A1 – *continued*

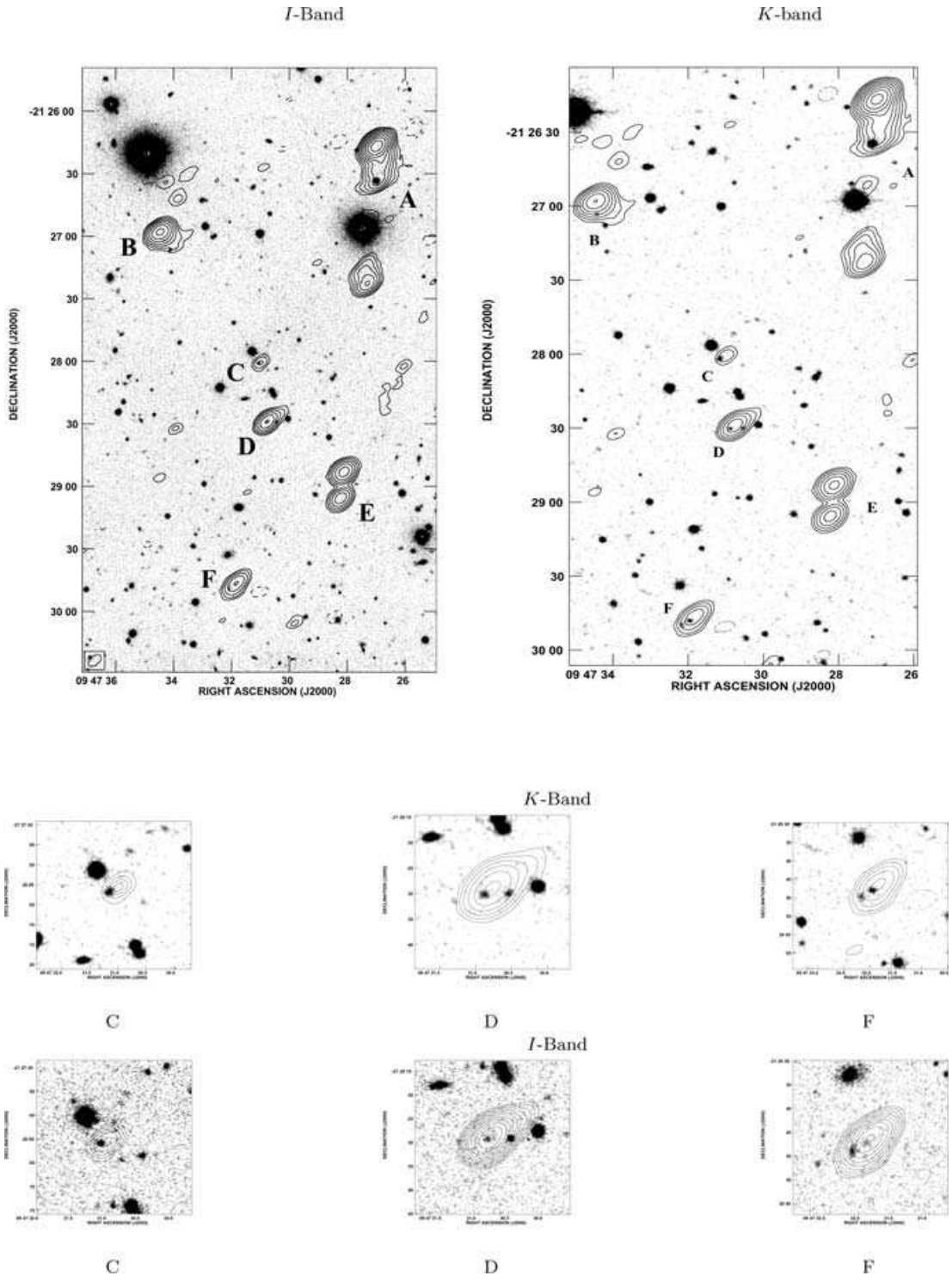

Figure A2. *I*-band (Paper 1) and *K*-band images (this work) of CENSORS 10, 90 and 103.

This paper has been typeset from a TEX/LATEX file prepared by the author.